NAVAL POSTGRADUATE SCHOOL
Monterey, California

THESIS

ANALYSIS OF LOW FREQUENCY TRANSMISSION
LOSS IN THE SHALLOW TIMOR SEA

by

Stuart M. Taylor

June 1999

Thesis Advisors:

Robert H. Bourke
James H. Wilson

Approved for public release; distribution is unlimited.

DTIC QUALITY INSPECTED 4

REPORT DOCUMENTATION PAGE

Public reporting burden for this collection of information is estimated to average 1 hour per response, including the time for reviewing instruction, searching existing data sources, gathering and maintaining the data needed, and completing and reviewing the collection of information. Send comments regarding this burden estimate or any other aspect of this collection of information, including suggestions for reducing this burden, to Washington headquarters Services, Directorate for Information Operations and Reports, 1215 Jefferson Davis Highway, Suite 1204, Arlington, VA 22202-4302, and to the Office of Management and Budget, Paperwork Reduction Project (0704-0188) Washington DC 20503.

1. AGENCY USE ONLY (Leave blank)	2. REPORT DATE June 1999	3. REPORT TYPE AND DATES COVERED Master's Thesis

4. TITLE AND SUBTITLE
Analysis of Low Frequencies Transmission Loss in the Shallow Timor Sea

5. FUNDING NUMBERS

6. AUTHOR(S) Taylor Stuart M.

7. PERFORMING ORGANIZATION NAME(S) AND ADDRESS(ES)
Naval Postgraduate School
Monterey, CA 93943-5000

8. PERFORMING ORGANIZATION REPORT NUMBER

9. SPONSORING / MONITORING AGENCY NAME(S) AND ADDRESS(ES)

10. SPONSORING / MONITORING AGENCY REPORT NUMBER

11. SUPPLEMENTARY NOTES
The views expressed in this thesis are those of the author and do not reflect the official policy or position of the Department of Defense or the U.S. Government.

12a. DISTRIBUTION / AVAILABILITY STATEMENT Approved for public release; distribution unlimited.	12b. DISTRIBUTION CODE

13. ABSTRACT (maximum 200 words)

The objectives of this study were to enhance understanding of the parameters affecting transmission loss in the shallow waters of the Timor Sea and to conduct a performance analysis of the range dependent acoustic PE model, RAM. The study utilised transmission loss data (from 10-1600 Hz) collected by DSTO and NAWC during the SWISS 1 experiment held in the Sahul Shelf area in early March 1994 in waters ranging from 60 to 120 m depth. In addition, transmission loss data from a similar experiment conducted in 1990 in the same area was used as a comparison to the SWISS 1 data.

The analysis revealed that the acoustic environment over the Sahul Shelf exhibits a high degree of lateral variability which is primarily dependent on the geological composition of the shelf region. Of particular interest was the north/south oriented SWISS 1 transmission loss data which displayed characteristics associated with shear wave coupling. RAM was able to accurately simulate the SWISS 1 transmission loss for regions uneffected by shear wave coupling but failed to simulate portions of the north/south track where transmission loss data was excessive. A version of RAM which incorporates shear wave effects, RAMS, was used to simulate the north/south transmission loss data. Due to the high range dependence of the geoacoustic parameters, coupled with inadequate availability of geoacoustic data for this region, only limited success was achieved using RAMS.

14. SUBJECT TERMS
Under Sea Warfare, Propagation Loss, Timor Sea, Shear Wave Coupling, Low Frequency Acoustic Transmission

15. NUMBER OF PAGES

16. PRICE CODE

17. SECURITY CLASSIFICATION OF REPORT Unclassified	18. SECURITY CLASSIFICATION OF THIS PAGE Unclassified	19. SECURITY CLASSIFI- CATION OF ABSTRACT Unclassified	20. LIMITATION OF ABSTRACT UL

NSN 7540-01-280-5500

i

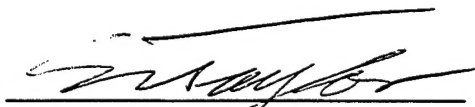# ANALYSIS OF LOW FREQUENCY TRANSMISSION LOSS IN THE SHALLOW TIMOR SEA

Stuart M. Taylor
Lieutenant Commander, Royal Australian Navy
B.Sc., University of New South Wales, 1984

Submitted in partial fulfillment of the
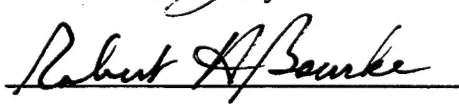requirements for the degree of

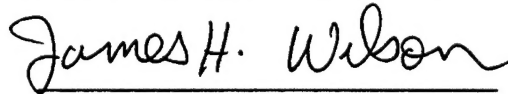## MASTER OF SCIENCE IN PHYSICAL OCEANOGRAPHY

from the

NAVAL POSTGRADUATE SCHOOL
June 1999

Author: _____
Stuart M. Taylor

Approved by: _____
Robert H. Bourke, Thesis Advisor

_____
James H. Wilson, Thesis Advisor

_____
Roland W. Garwood, Chairman
Department of Oceanography

ABSTRACT

The objectives of this study were to enhance understanding of the parameters affecting transmission loss in the shallow waters of the Timor Sea and to conduct a performance analysis of the range dependent acoustic PE model, RAM. The study utilised transmission loss data (from 10-1600 Hz) collected by DSTO and NAWC during the SWISS 1 experiment held in the Sahul Shelf area in early March 1994 in waters ranging from 60 to 120 m depth. In addition, transmission loss data from a similar experiment conducted in 1990 in the same area was used as a comparison to the SWISS 1 data.

The analysis revealed that the acoustic environment over the Sahul Shelf exhibits a high degree of lateral variability which is primarily dependent on the geological composition of the shelf region. Of particular interest was the north/south oriented SWISS 1 transmission loss data which displayed characteristics associated with shear wave coupling. RAM was able to accurately simulate the SWISS 1 transmission loss for regions uneffected by shear wave coupling but failed to simulate portions of the north/south track where transmission loss data was excessive. A version of RAM which incorporates shear wave effects, RAMS, was used to simulate the north/south transmission loss data. Due to the high range dependence of the geoacoustic parameters, coupled with inadequate availability of geoacoustic data for this region, only limited success was achieved using RAMS.

TABLE OF CONTENTS

ACKNOWLEDGEMENT

I. INTRODUCTION

Currently, a dichotomy exists as medium and small maritime forces face tighter budget constraints while at the same time the cost of the modern and sophisticated weapons and sensors required to effectively perform designated roles continues to rise. If these maritime forces are to ensure adequate and timely surveillance of their areas of operation, they need to maximise/optimise the use of the weapons and sensors that they have available to them. To achieve optimum performance from such weapons and sensors, full cognisance of the impact exerted by the environment on these devices needs to be taken into account. This is particularly important for the Royal Australian Navy, which has a vast surveillance area and limited resources.

The Under Sea Warfare (USW) component of a Maritime Force's mission is particularly dependent on the prevailing environmental conditions. The high spatial and temporal variability of the three dimensional water column/sediment distribution and the sound speed temporal/spatial variability in each medium requires the user to have a well founded knowledge of their operating environment. Collecting and analysing the required data fields to ensure an appropriate level of knowledge about the desired USW operating areas is both time consuming and expensive. Inversion techniques (IT) offer a relatively inexpensive and timely means of developing an adequate understanding of the USW environment. Every USW sonar can assist in characterising the environment using ITs. Different sonars help paint differing 'pictures' of the environment. Higher frequency sonars can yield information concerning bottom sediment/clutter interface resolution while lower frequency sonars can provide a three dimensional estimate of the

sediment volume characteristics. Two previous studies, Scanlon et al. (1995) and Null et al. (1996), have shown the value of utilising ITs to infer sedimentary characteristics.

In order to achieve a greater understanding of the Australian USW environment, the Maritime Operations Division of the Defence Science and Technology Organisation (DSTO), Salisbury, Australia, in collaboration with the Naval Air Warfare Center (NAWC), Warminister, Pennsylvania, conducted a series of trials in the northwest waters (Timor Sea) of Australia in 1994. One such trial, the Shallow Water In Situ Survey (SWISS), was designed to support ongoing research to measure and understand those environmental parameters that affect shallow water sonar performance as well as verifying acoustic models needed to predict sonar system performance. The major objectives of the trials were to determine bistatic reverberation, acoustic transmission loss, onmidirectional ambient noise, ocean current and DICASS reverberation, transmission loss and pulse envelopes (Larsson et al., 1994).

This thesis will focus on the transmission loss data recorded in the Timor Sea during SWISS 1. The objective of the thesis is to use IT-style analysis to gain a better understanding of the parameters affecting transmission loss and conduct a performance analysis of the full wave parabolic equation model, RAM, in the SWISS 1 environment.

An additional transmission loss experiment was conducted earlier in the same area in 1990 and will be used to augment the data collected during SWISS 1. This experiment was conducted using the Royal Australian Navy's former research vessel HMAS COOK (Carter et al., 1992) and provides interesting and supporting comparisons to the SWISS 1 trial data.

II. SHALLOW WATER IN-SITU SURVEY NO 1

The SWISS 1 survey was conducted on 5 March 1994 on the Timor shelf off the northwest coast of Australia (Figure 1). The experimental procedures have evolved during a series of similar trials that were initially designed by NAWC.   The measurement procedure was called the NAWC Harsh Environmental Program 'HEP" and during SWISS 1 was conducted by a single Royal Australian Airforce (RAAF) P3C. The aim of the transmission loss part of the survey was to measure the loss in one-third octave bands at a site in two orthogonal directions (Larsson et al., 1994). The equipment used is detailed in Table 1.

Equipment Type	Purpose
Airborne expendable bathythermographs(AXBT)	Record temperature profile
Type 57A sonobuoys	Record signal noise level
AQH4 tape	Recording medium
Hp 3562A Dynamic Signal Analyser	Digitiser
820 g SUS charges	Sound source

Table 1. Equipment used for SWISS 1 (Larsson et al., 1994)

A.   EXPERIMENTAL PLAN

Five positions, five nm apart, all lying in a line were identified and called posts A1 through A5 (Figure 2).   Initially the P3C dropped multiple hydrophone receivers (sonobuoys) in a cluster at posts A1, A3 and A5, as well as an AXBT on the first run. AXBTs were dropped regularly around the trial site to measure the temperature profile. Three reverberation measurement runs were conducted followed by two transmission loss runs. For the transmission loss runs the P3C dropped a SUS charge every nautical mile along a strait line path emanating from posts A3 and A5 (Figure 3). The first run was a
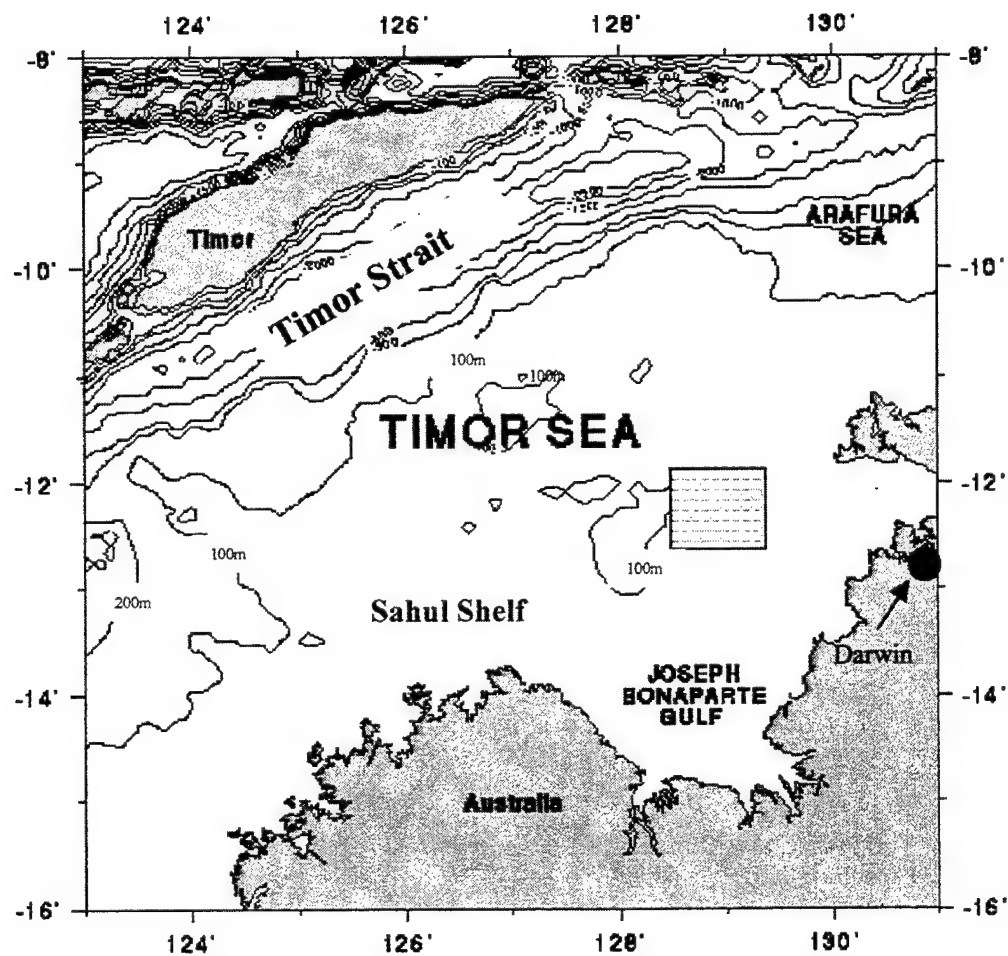
3

Figure 1. Timor Sea. The SWISS 1 experimental area is indicated by the shaded box. (http://www-ocean.tamu.edu/~baum/paleo/seamaps/timor-sea.gif)
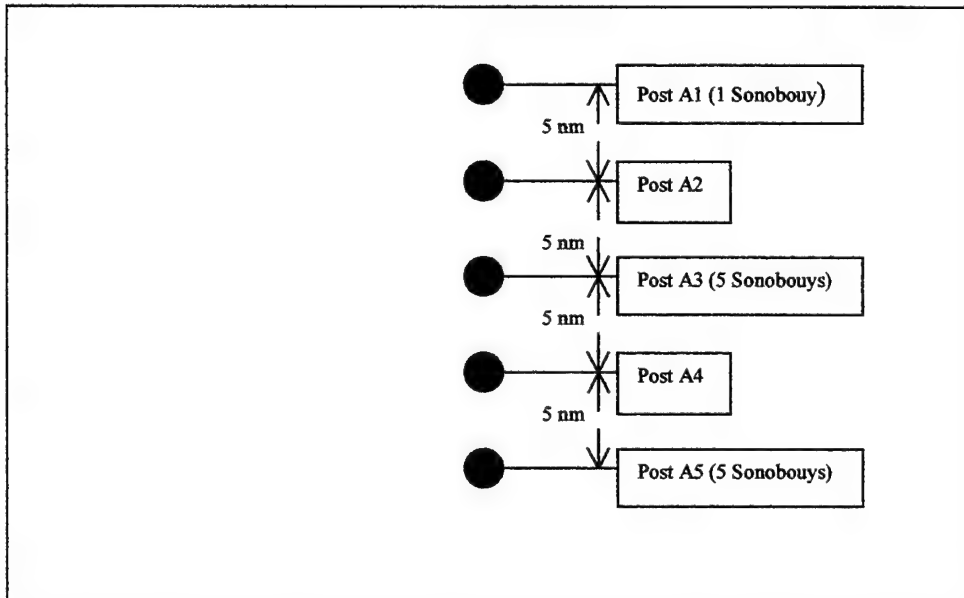
4

Figure 2.   SWISS 1 trial posts (Larsson et al., 1994).

25 nm run south of post A3 while the second was a 15 nm run to the west of a post A5 (Figure 3). The total energy received from each SUS charge, as measured at post A3 for the north/south run and at A5 for the east/west run, was calculated in one-third octave bands and subtracted from the source strength of the SUS charge. The result was recorded as the transmission loss. The transmission loss value used was taken from the hydrophone which exhibited the least attenuation (i.e., had the highest received signal level) and that was not saturated by the SUS charge. No averaging of the received signal level from each sonobuoy was performed nor was the variability of the received signal level established. The source strength of the SUS charges was determined using the procedures of Weston (1960) and were calculated by M. Hall of DSTO (Larsson et al., 1994). The SWISS 1 experiment was completed during a period of several hours so that assumptions related to minimal temporal variability of environmental parameters are well founded.

B.   ENVIRONMENT

1.   Timor Sea

The Timor Sea lies between northwestern Australia and Timor and consists of the Timor Strait and Sahul Shelf (Figure 1). The shelf is a shallow water region that occupies about two thirds of the area of the Timor Sea. The SWISS 1 trial was conducted on the shelf approximately 150 nm to the west of Darwin where the water depth varied from 60 to 120 m, deepening to the south and west (Figures 4a and 4b).

The experimental region lies within the monsoonal region of Australia. The southeast monsoon (dry monsoon) occurs from November through March and the

6

SWISS 1 Surface Sediment Compressional Wave
Speed Contour Map
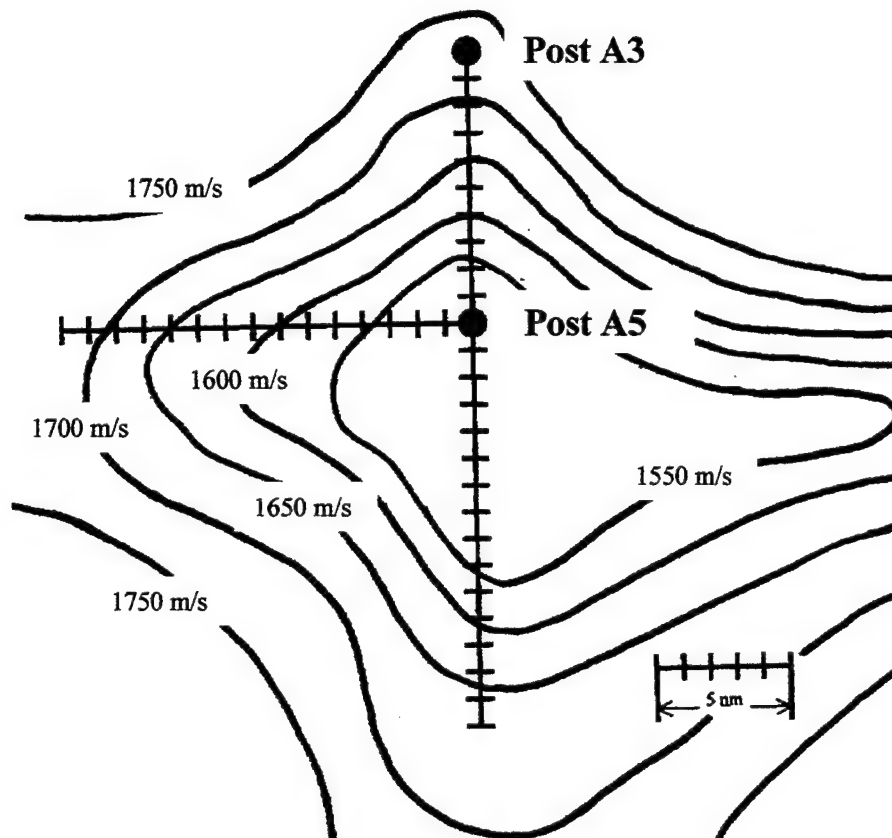
Figure 3.   Schematic of SWISS 1 exercise plan showing east/west and north/south transmission loss runs.   Contours indicate 50 m/s intervals in surface sediment compressional wave speed.   Both SWISS 1 runs are indicated by the vertical and horizontal lines.   Each mark on the run lines indicates position of each SUS charge dropped by the P3C.

E/W Bathymetry and Surface Sediment Composition

(a)

Silt   Silty Sand   Very Fine Sand   Fine Sand

N/S Bathymetry and Surface Sediment Composition

(b)

Fine Sand   Very Fine Sand   Silty Sand   Silt
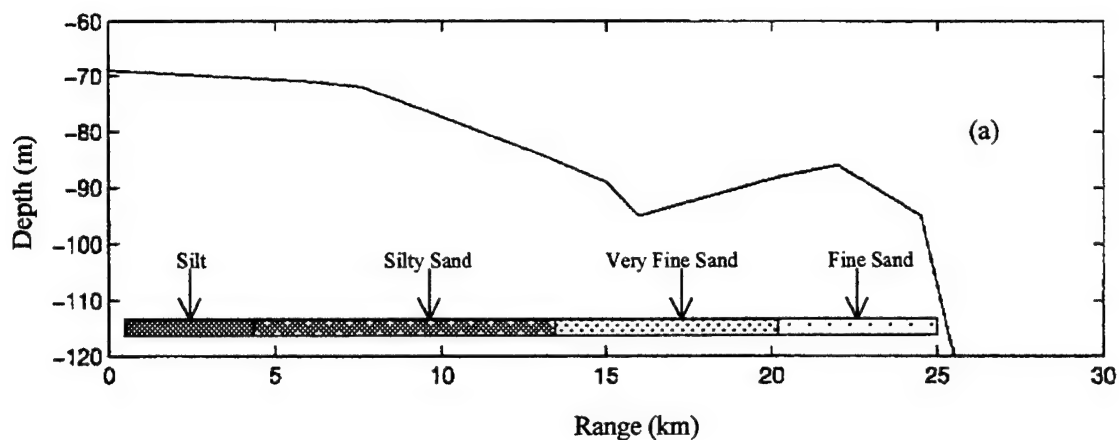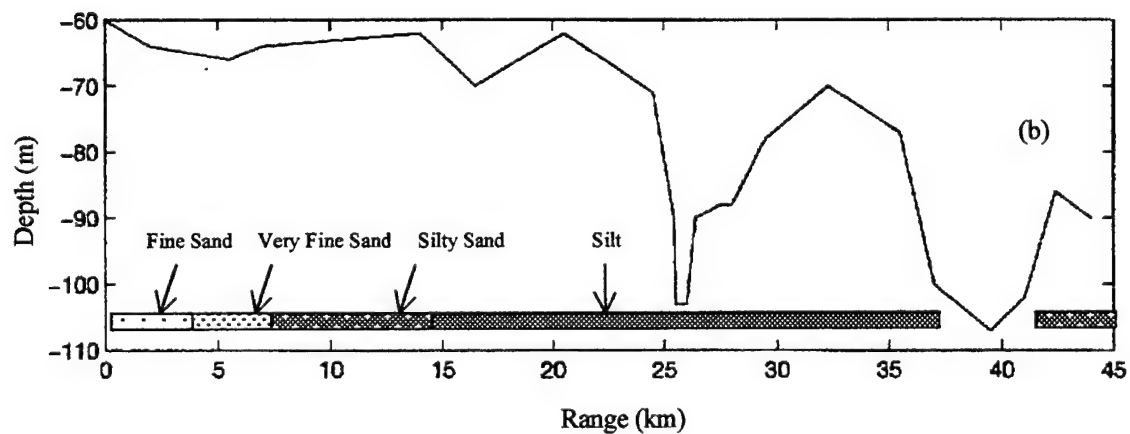
Figures 4a and 4b. Bathymetry along the (a) east/west and (b) north/south SWISS 1 runs. The surface sediment composition along each path is displayed at the bottom of each figure.

8

northwest monsoon (wet monsoon) occurs from May through September. March is usually the beginning of the transition period between the northwest and the southeast monsoon season (BOM, 1994). The synoptic situation for March 1994 began with the monsoon trough situated south of the Sahul Shelf. The monsoon trough weakened considerably during the first week of March and moved north of the experimental area, such that meteorological parameters were essentially benign during the conduct of SWISS 1. The temperatures and rainfall amounts for March 1994 were generally about average (BOM, 1994). The local wind speed at the time of the trial was measured as 2.5 m/s (5 knots) at 133 m above sea level and extrapolated to the surface as 1 to 2.5 m/s (2 to 5 knots) (Larsson et al., 1994).

Currents on the shelf display a distinct cycle linked to the changing wind field of the monsoons. During the southeast monsoon (May-September) the surface flow across the shelf is to the west. During the northwest monsoon (November-March) the flow weakens and even reverses direction over the inshore part of the shelf. Current speeds are slow during both seasons varying between 0.1 and 0.3 m/s (Creswell et al., 1993).

The sound speed profile was deduced from the temperature profiles that were regularly recorded by AXBTs throughout duration of the experiment (Figure 5). The profile shape remained essentially unchanged throughout the period of the trial (Larsson et al., 1994). The profile shows no surface duct but a weak 30 m layer that is nearly isospeed. The profile below the layer is that of an isothermal layer. Although these features can be deduced from the sound speed profile, the water column as a whole can

9

be treated as isospeed because the greatest variation in sound speed is only 1 m/s throughout the entire water column.

2.   Geology

Noting the benign weather conditions, it is reasonable to expect that the water column and atmospheric conditions would exert little temporal or spatial variability on acoustic transmission loss. With this in mind, particular attention was paid to the nature of the geologic and sediment characteristics as possible causes of anomalous acoustic transmission loss.

Although the Timor Sea is a significant oil and gas region, little geoacoustic data is available concerning the first 500 m of the sediment throughout the Sea. The geology and deep sediment structure are well studied in the areas that are believed to contain economical oil and gas reserves (Winter, 1998). However, little is known concerning the SWISS 1 area because it lies to the southeast of the known oil and gas fields (Winter, 1998; Strickland, 1999).

The Timor Sea has a complex structural history and consists of a number of Paleozoic and Mesozoic sub-basins and platforms. Initial rifting took place in the Late Devonian to Early Carboniferous with the development of the northwest trending Petrel Sub-Basin which contains the SWISS 1 area. Further rifting occurred which ultimately led to the break up of Gondwanaland (O'Brien and Woods, 1995).

Following continental breakup, widespread shelfal marine environments were established by the Paleocene. Deposition of carbonates with minor sandstones continued from the Paleocene to the present day. The collision of the Australian and Eurasian Plates in the Late Miocene to Early Pliocene resulted in the partial to complete breaching
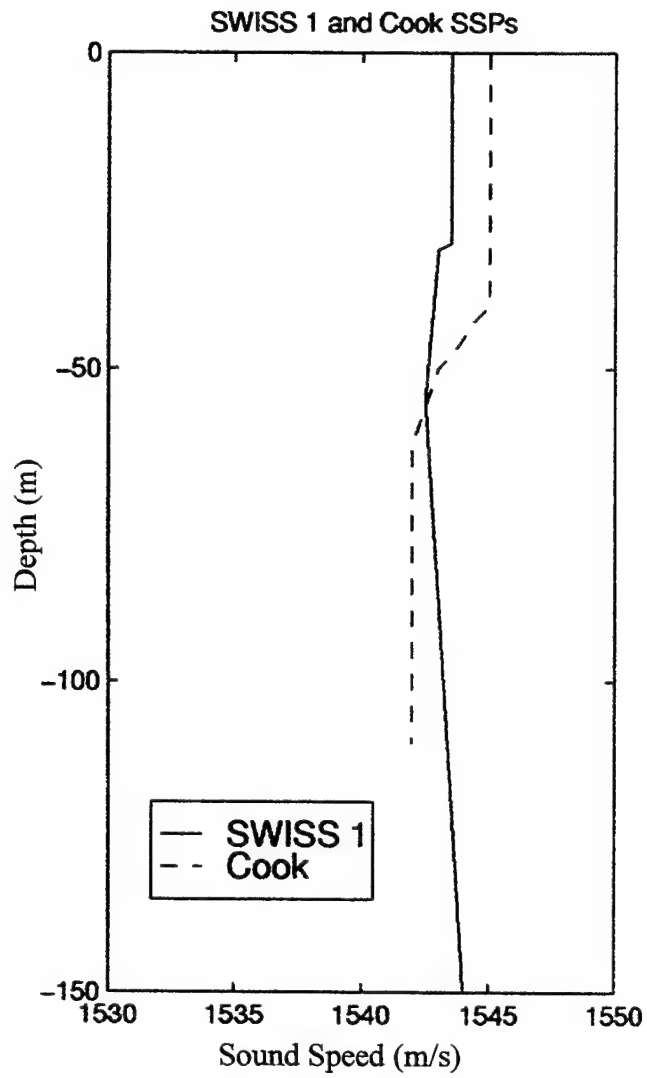
10

Figure 5. Sound speed profiles (SSP) for the SWISS 1 and Cook experiments (Larsson et al., 1994; Carter et al., 1992).

of many charged hydrocarbon traps and facilitated the vertical migration of hydrocarbons (O'Brien and Woods, 1995).

Bishop and O'Brien (1998) identified several anomalous seismic reflections in the shelf area immediately to the west-northwest of the SWISS 1 area. The shape of these anomalies is described as an inverted 'Christmas Tree'. The central core of the anomalies is characterised by chaotic reflectors with quite variable and occasionally high amplitudes. These anomalies are believed to be created by the presence of light hydrocarbons, such as gas and/or light condensate within the sediment. The core represents sediment that has been disturbed by the passage of gas. Fault movements and gravity sliding may exacerbate the observed deformation within the core. In some of the cores, zones of high acoustic speed have been observed. Bishop and O'Brien (1998) suggest that these zones may have been created by cementation of the sediment with diagenetic carbonate, which was produced via the oxidation of hydrocarbons passing through the sediment. This cementation can produce the very high speed zones within the core of the gas chimney. O'Brien and Woods (1995) have documented a similar process in the deeper sediments in the shelf areas to the southwest. Although there is no geologic evidence that proves the presence of these high speed features in the SWISS 1 area, their existence can not be discounted (Strickland, 1999).

Sahul shelf sediments are largely coarse-grained mixtures of gravel and sand with mud. The majority of mid to outer shelf bathymetric rises and inner shelf zones are dominated by a combination of carbonate sands and gravels. Coarse calcareous sands also dominate the outer shelf banks. Gravels

12

are absent from shelf deposits only in the Bonaparte Depression. The carbonate sand is derived from molluscs, corals and planktonic foraminifers (Sendt, 1999).

This thesis utilises surface sediment data provided by DSTO which were determined using a technique devised for DSTO by the Ocean Sciences Institute of the University of Sydney (Jones, 1998). The data included surface porosity, compressional wave speeds, relaxation time, phi size, sorting and some limited shear wave speeds. Comparison of the sediment surface data provided by DSTO and those sediment parameters defined in Hamilton's Table II (Hamilton, 1982) indicated that the sedimentary environment contained fine sand, very fine sand, silty sand and silt regimes (Figures 4a and 4b). Due to the general lack of geoacoustic data within the area of interest and advice that the basement rock lies from 500 m to 1000 m below the sediment surface (Strickland, 1999), the sediment was assumed to be 500 m thick. The presence of consolidated sedimentary material, i.e., highly reflective cemented sediment, within the experimental area was not discounted.

C.   TRANSMISSION LOSS DATA

Figures 6a and 6b show the SWISS 1 measured transmission loss plots for one-third center band frequencies ranging from 80 Hz to 1250 Hz for the east/west and north/south runs, respectively. Contour plots of the transmission loss as a function of range over the frequency span of 10 Hz to 1600 Hz are displayed in Figures 7a and 7b. These figures indicate that considerable difference in transmission loss is observed between the two runs.

1.   East/West Run

For all frequencies the transmission loss decays at a rate which is slightly less than spherical (20 log r) but still is significant, reaching 85-90 dB at 25 km (Figure 6a). The rate of loss is fairly uniform over the recorded 25 km path.   The frequency/loss relationship displayed indicates that 200 Hz is the optimum frequency for this specific environment.   The high losses for frequencies below 200 Hz may be indicative of leakage losses, e.g., 80 Hz.   Frequencies above 200 Hz display a frequency/loss relationship that can be associated with scattering/absorption effects.

2.   North/South Run

The transmission loss is significantly greater than spherical for all frequencies along the north/south path with the loss exceeding 110 dB at 44 km for the majority of frequencies (Figure 6b).   The rate of loss is initially severe, approaching 40 log r, until approximately 13-15 km at which point the rate of loss moderates to about 20 log r.   The transmission loss data also shows a high degree of frequency dependence from that point on. That is, the majority of loss occurs between 80 Hz and 250 Hz (Figure 7b).   This frequency dependence is significant as it may indicate energy bleeding through shear wave propagation (Ellis and Chapman, 1985; Jensen, 1991).   High attenuation below 200 Hz in shallow water has been attributed to shear wave coupling as a result of consolidated material occurring near the water-sediment interface.   This effect will be further discussed in Section B, Chapter IV.
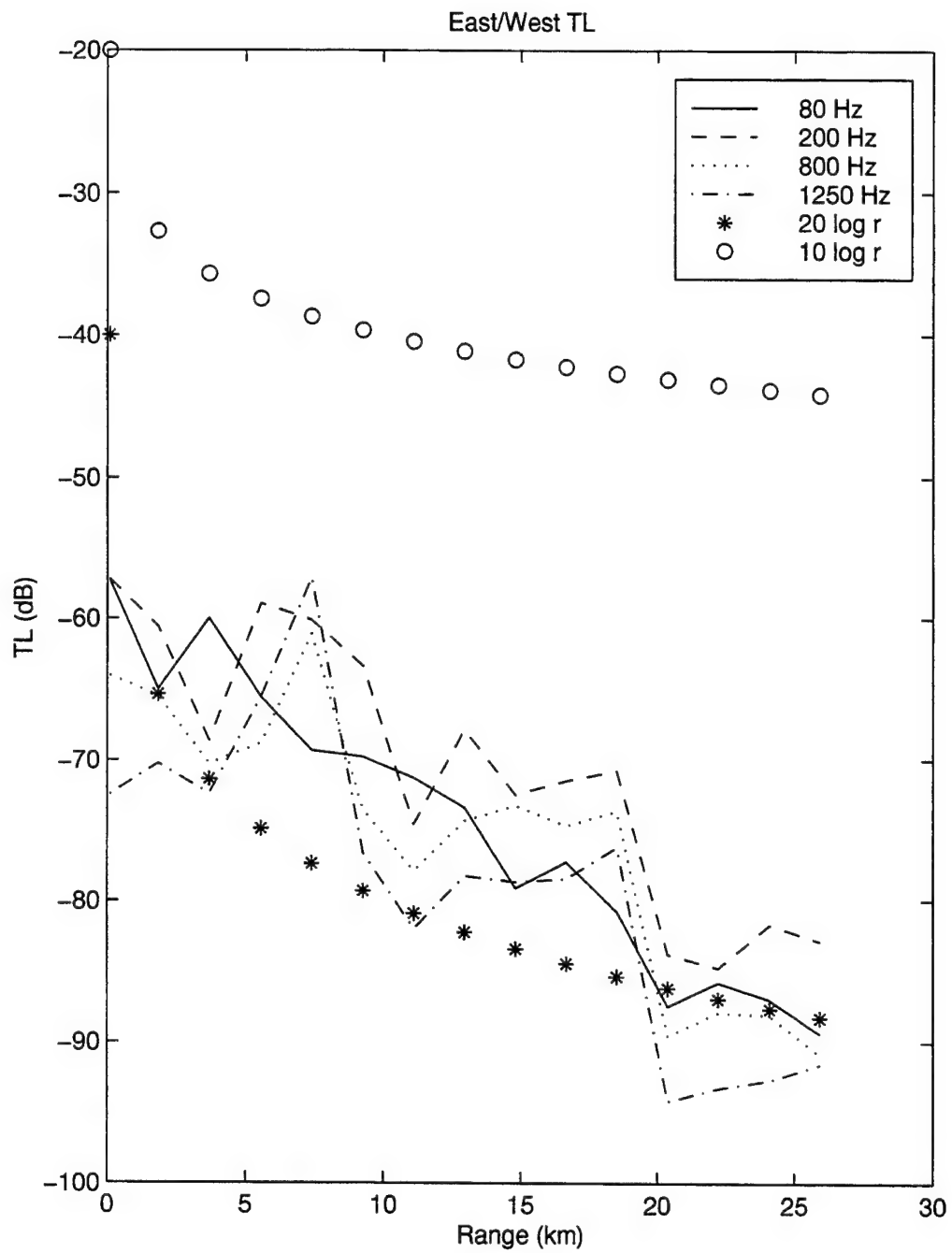
Figure 6a. East/west SWISS transmission loss data vs range. Spherical (20 log r) and cylindrical (10 log r) spreading have been plotted for comparison.

15
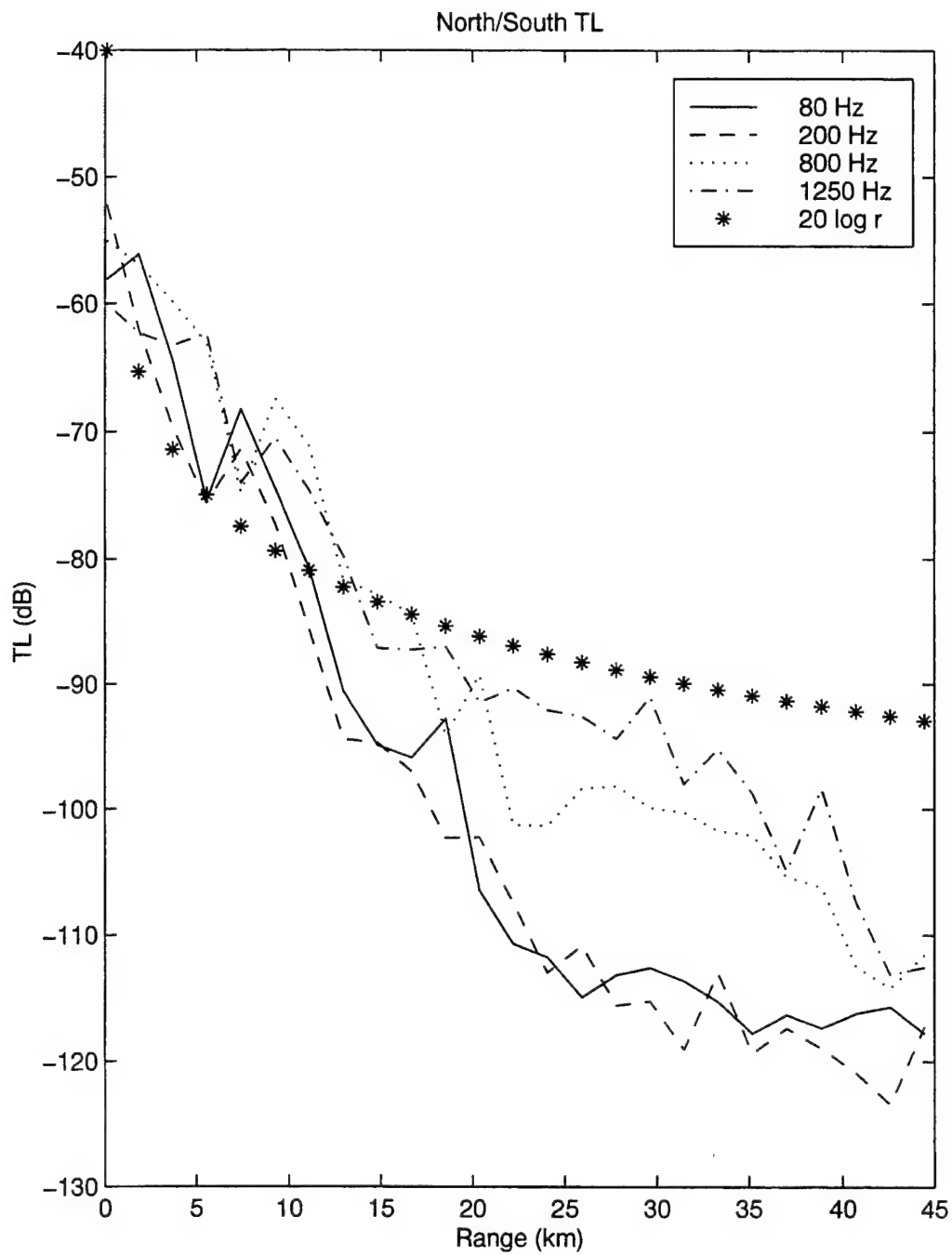
Figure 6b. North/south SWISS 1 transmission loss data vs range. Spherical (20 log r) spreading has been plotted to provide a comparison.

16

E/W TL

Legend:
☒ 40-45 ☒ 45-50 ☐ 50-55 ☐ 55-60 ☐ 60-65 ☒ 65-70 ☐ 70-75 ☐ 75-80
☐ 80-85 ☐ 85-90 ☒ 90-95 ☐ 95-100

Figure 7a. East/West transmission loss. Warm colours represent high loss and cool colours represent low loss in increments of 5 dB.

N/S TL

Figure 7b. North /South transmission loss. Warm colours represent high loss and cool colours represent low loss in increments of 5 dB. Of particular interest is the band of high loss from 40-250 Hz.

18

III. COOK TRANSMISSION LOSS EXPERIMENT

Carter et al. (1992) conducted a transmission loss experiment in approximately the same region of the Timor Sea as the SWISS 1 trial during 1990, four years prior to SWISS 1. The procedure used in this experiment was similar to that used in the SWISS 1 trial therefore providing an opportunity for intercomparison of the data from the experiments.
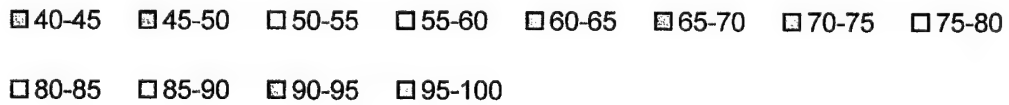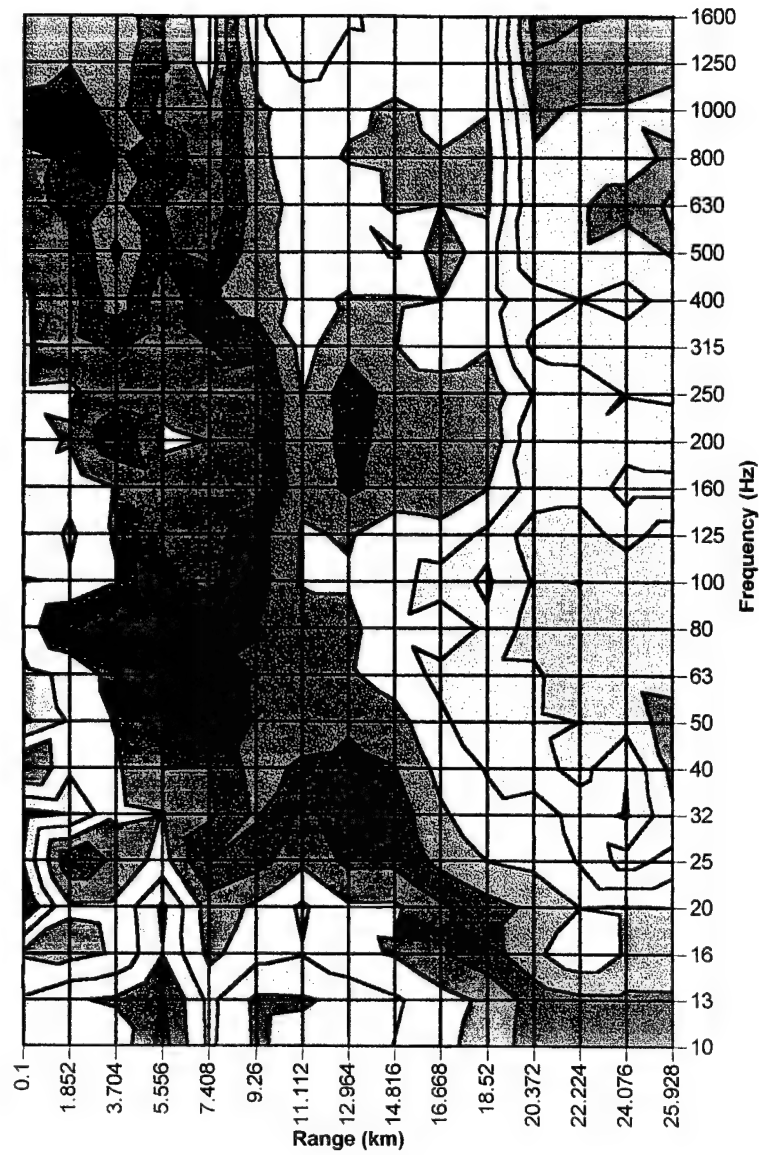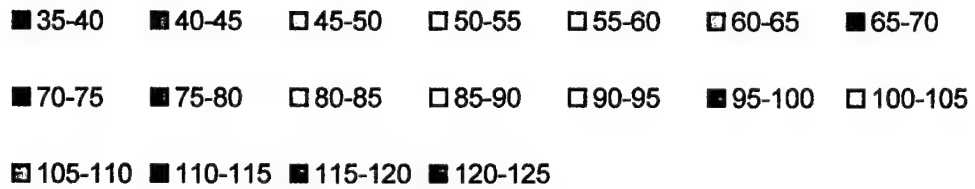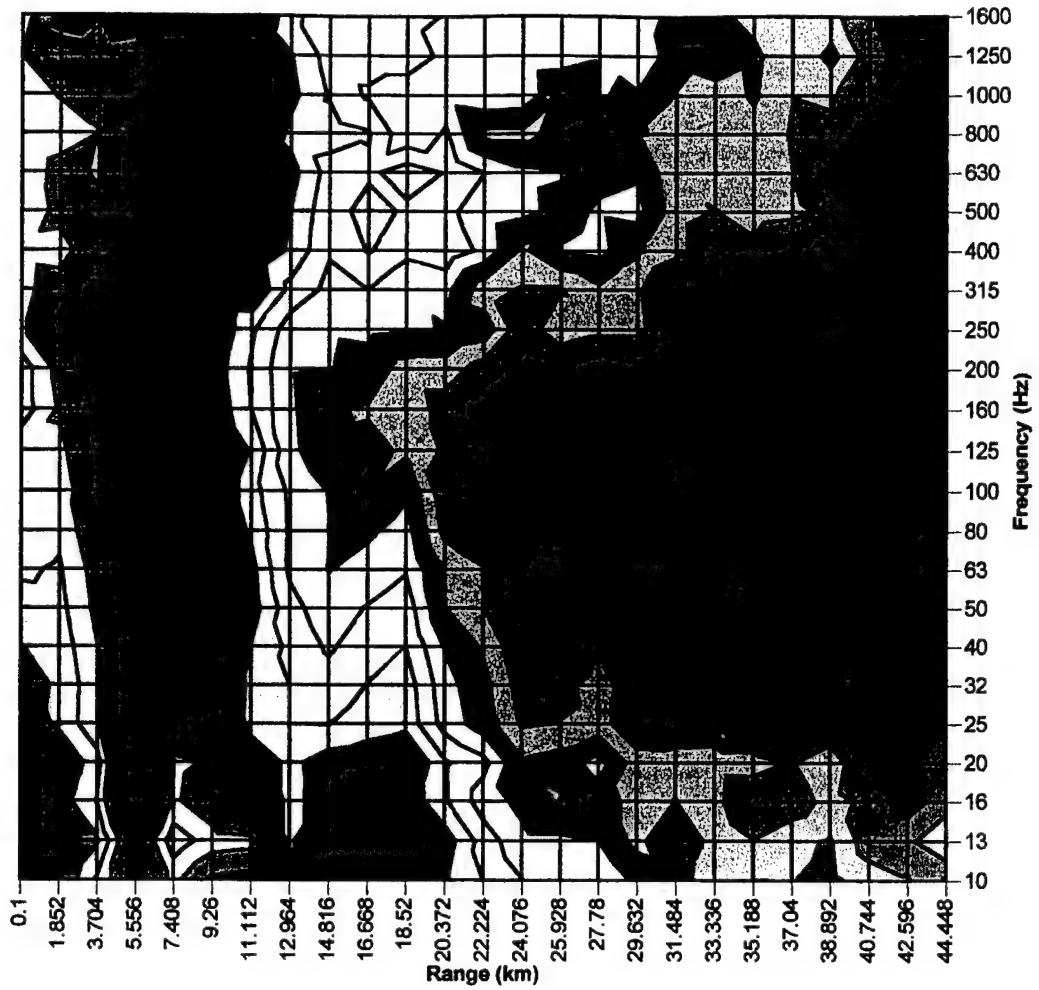
The significant differences between the two experiments were;

a. The former Royal Australian Navy Oceanographic vessel, HMAS COOK, was used as the experiment platform instead of a P3C.

b. Smaller Mk 64 (31g) SUS charges were used instead of 820 g charges.

c. Type SSQ-41B sonobuoys were used instead of the type 57A sonobuoys used in SWISS 1.

Analytical determination of source level values for a 31 g SUS charge is difficult because Weston's (1960) method for scaling the source spectrum level of a large to a small SUS charge has resulted in significant discrepancies at low frequencies (Carter et al., 1992). To avoid any discrepancies the source levels used in the COOK experiment were those measured by Thorleifson and Boyle (1976) for a 31 g charge detonated at a depth of 18 m over the frequency band 10 Hz to 1600 Hz (Carter et al., 1992). Comparison of the source level values used in the COOK experiment to those used in SWISS 1 show that the energy spectral densities (J/steradian/Hz) of the 31 g charge are approximately one tenth that of the 820 g charge (Carter et al., 1992; Jones, 1993).

19

The relative environments of the two sites were quite similar particularly the water depth, sound speed profile (Figure 5) and current weather conditions. A comparison of the relative sediment compositions, especially vertical gradients of geoacoustic properties, was not possible due to lack of sediment data available for each experiment.

The transmission loss data for the COOK trial are shown in Figures 8 and 9. There is no indication of the bandwidth filtering that was observed in the north/south SWISS 1 run. The transmission loss is more conventional with the loss increasing monotonically with frequency. The clustering of the transmission loss curves around the spherical spreading curve indicates that this is a region of high bottom attenuation.

A comparison of the SWISS 1 trial results and the COOK data is shown in Figures 10 a through 10 f. Of note is that at the lower frequencies ($\leq$315 Hz) the COOK data closely resembles the east/west SWISS 1 data. At higher frequencies ($\geq$800 Hz) the COOK data demonstrates losses which exceed that recorded by both the SWISS 1 runs. Carter et al. (1992) offer no explanation for the very high losses above 500 Hz.
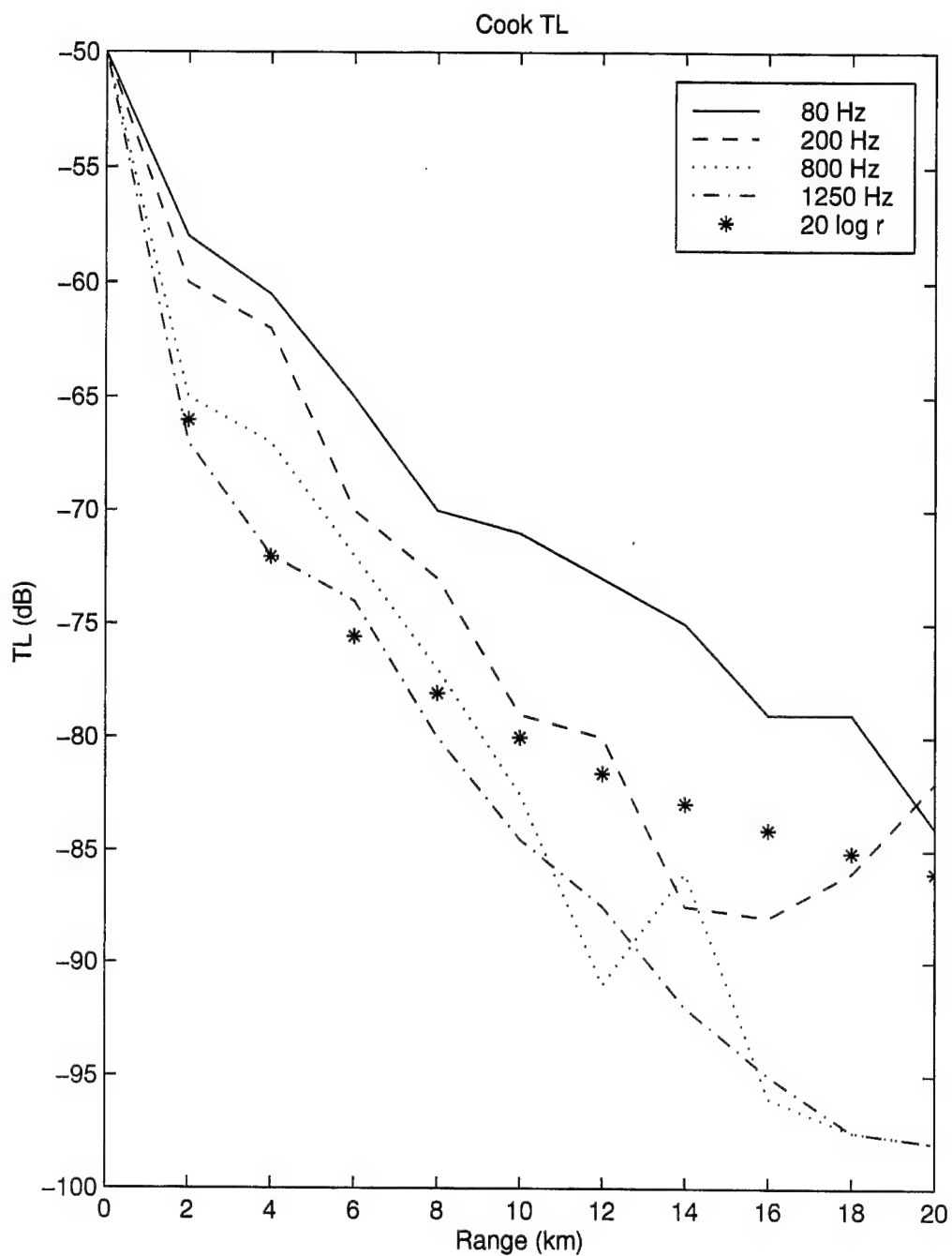
Figure 8. COOK transmission loss data vs range. Spherical (20 log r) spreading has been plotted to provide a comparison.
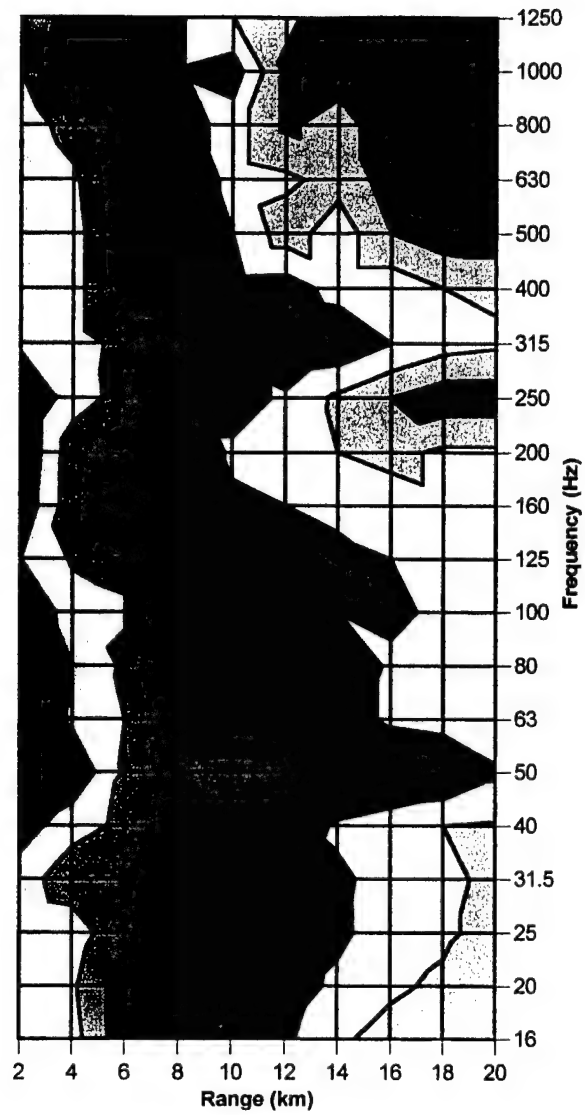
Figure 9. Cook transmission loss. Warm colours represent high loss and cool colours represent low loss in increments of 5 dB.
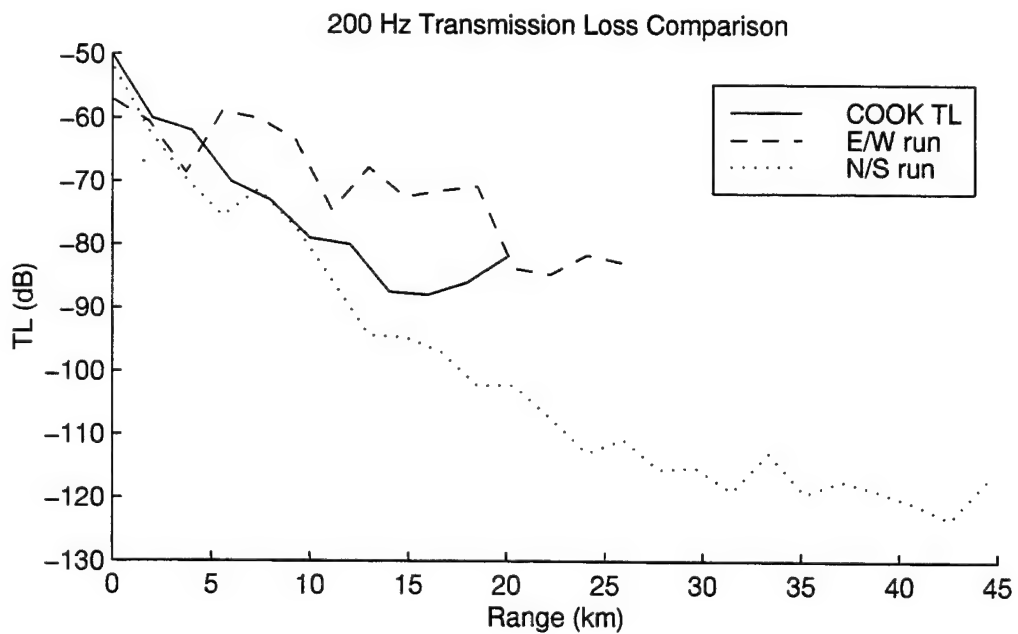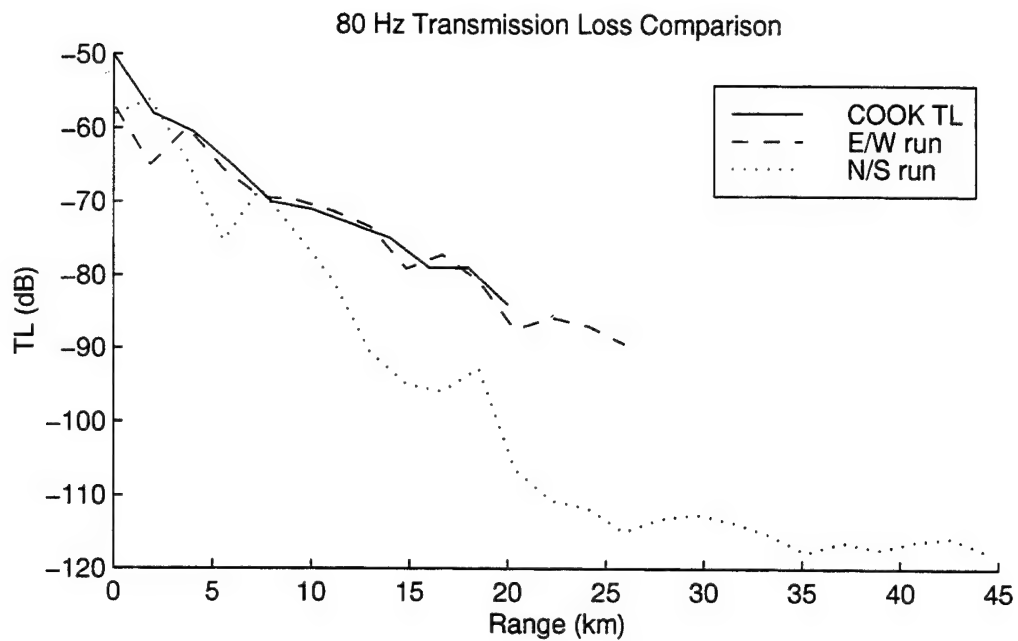
Figures 10a and 10b. A comparison between the east/west, north/south SWISS 1
transmission loss data and the COOK transmission loss data for (a) 80 Hz
and (b) 200 Hz.

23
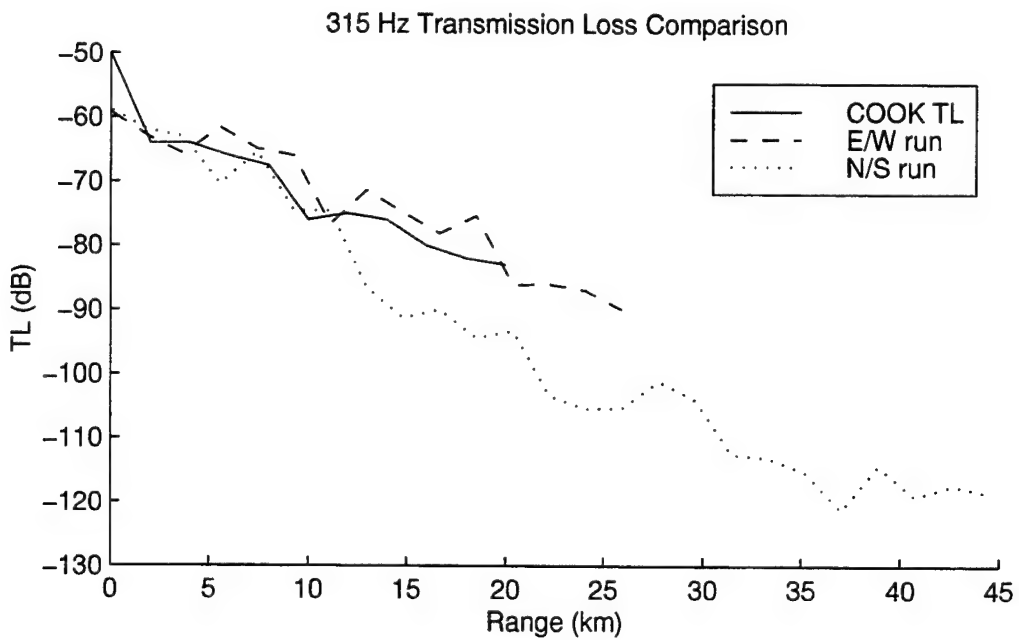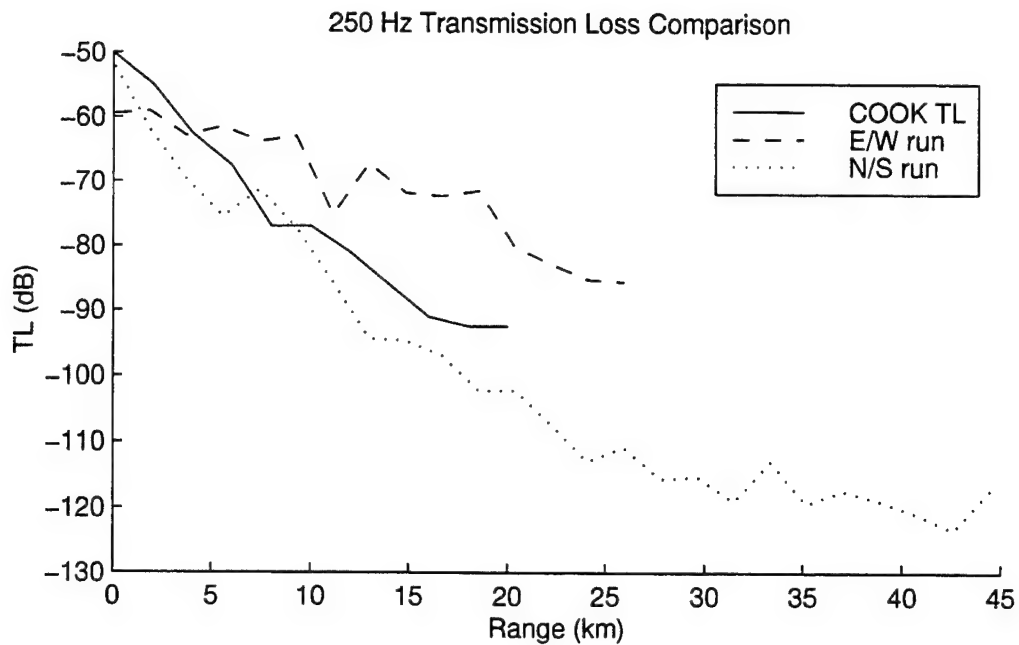
Figures 10c and 10d. A comparison between the east/west, north/south SWISS 1
transmission loss data and the COOK transmission loss data for (a) 250 Hz
and (b) 315 Hz.

24
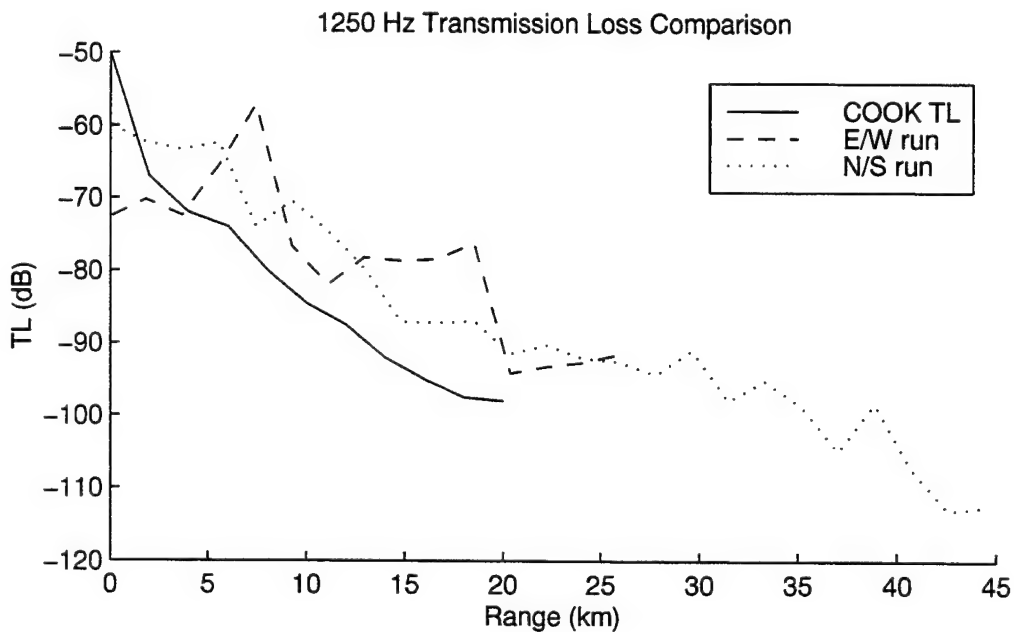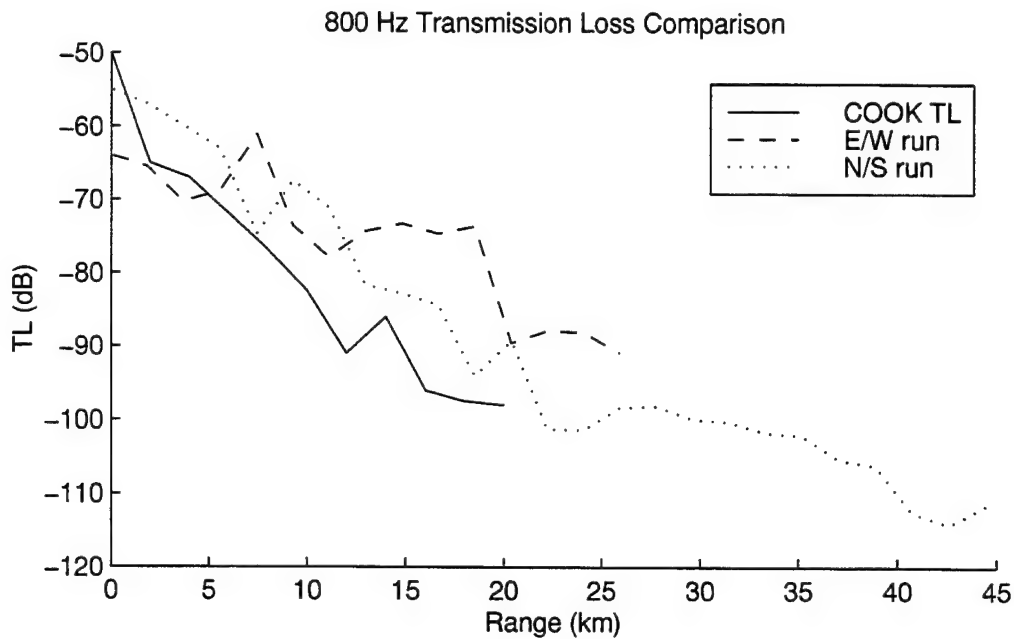
Figures 10e and 10f.   A comparison between the east/west, north/south SWISS 1 transmission loss data and the COOK transmission loss data for (a) 800 Hz and (b) 1250 Hz.

25

THIS PAGE INTENTIONALLY LEFT BLANK

IV. GEOACOUSTIC AND ACOUSTIC MODELING TECHNIQUES

If USW weapons and sensors are to be utilised to their optimum capability, then the performance of these weapons and sensors within the operating environment must be accurately predicted.   Central to this is knowledge of the geoacoustic environment as the seabed is known to be the controlling factor in low frequency shallow water acoustics. A lossy seabed causes attenuation of waterborne sound due both to a critical angle effect and to the attenuation of compressional waves in the seabed material (Jensen, 1991).   In order to effectively model acoustic propagation in shallow water the seabed needs to be modeled via a geoacoustic model; simple bottom reflection models have proven to be inadequate.

A.   GEOACOUSTIC MODEL

A geoacoustic model is defined as " a model of the real sea floor with emphasis on measured, extrapolated and predicted values of those properties important in underwater acoustics and those aspects of geophysics involving sound transmission. In general, a geoacoustic model details the true thickness and properties of sediment and rock layers in the sea floor" (Hamilton, 1980, p. 1313).

Due to the wide range of sediment compositions and distributions found in marine sediments the mechanical and acoustic properties of sediments can vary greatly.   In nearshore environments this spatial variability may be extreme, often changing on spatial scales of 10 km or less.   A large number of physical parameters are involved. Of these, the more important are porosity; grain properties including size, shape and sorting; elastic moduli; density and inter-granular stresses involving grain interlocking and consolidation.   Of most interest to underwater acoustics are the compressional wave

27

speed and attenuation, characteristic acoustic impedance, and shear wave speed and attenuation (Dunlop, 1992). Some of these parameters, such as porosity and wave speed, can be directly measured in-situ while others are inferred using a variety of relationships such as Hamilton's (1982) regression equations.

Hamilton's regression equations were used to determine the values of density and attenuation and their variation with respect to sediment depth (Hamilton, 1980). The attenuation at the sediment surface was calculated using the porosity values provided by DSTO and Figure 18 of Hamilton (1980). The attenuation versus depth relationship was determined using Figure 20 of Hamilton (1980). Surface density was also determined from the porosity based on an expression by Hamilton and Bachman (1982):

$$n = 157.6 - 57.8\,\rho$$

where n = porosity (%) and ρ = density (g/cm^3).

The density verses depth relationship was derived from Figure 22 of Hamilton (1980).

The compressional wave speed gradient was determined based on a modification of Carlson et al.'s (1986) procedure. Hamilton's (1985) procedure was deemed inappropriate for this region as described below. Carlson et al. (1986) conducted a correlation analysis on 233 sets of sediment data collected by the Deep-Sea Drilling Project in an attempt to establish depth/time and depth/speed relationships. The analysed data represented a wide range of physiographic and geologic provinces: mid-ocean ridge flanks, abyssal plains, back arc basins, oceanic plateaus, turbidite fans, continental slopes and a few seamounts. Carlson et al. developed a well constrained empirical model for the variation of wave speed with depth based on the assumption that the compressional

28

wave speed increased exponentially with depth. The best fitting equation for the speed/depth relationship was:

$$V = 1.58 \exp (0.33Z)$$

where V = compressional speed (km/s)

and   Z = depth of sediment (km)

While this equation represents a well constrained model for a large range of geological provinces, the validity of it has not been assessed in relation to continental shelves due to lack of data (Carlson et al., 1986).

Larsson (1994) conducted an analysis of Carter et al.'s (1992) earlier experimental results in the Timor Sea and concluded that Hamilton's compressional wave speed regression equations where not appropriate for northern Australian waters. He offered two possible reasons for this:

a.   The Timor Sea mean grain size distribution displays a lack of silt compared to Hamilton's definition, and

b.   The regression equations do not consider the underlying structure of the seabed.

Larsson (1994) suggested that a modified version of Carlson et al.'s (1986) relation would be more appropriate, namely:

$$V_c(d) = V_c(0) \exp (0.33 * d)$$

where $V_c(0)$ = the sediment compressional wave speed at the sediment/water

interface

and $V_c(d)$ = the wave speed at sediment depth 'd'.

This version differs only in that it allows for a user selected value for $V_c(0)$; it is not a universal constant as implied by using 1.58 km/s.

Larsson highlights that, although this model does provide significant improvement in the predicted transmission loss data compared with Carter et al's. (1992) measured propagation loss data, it fails to produce a close correlation between the predicted and measured data. As a result of problems encounted by herself and others, Sendt (1999) strongly recommended that Larsson's model be adopted for the purposes of this analysis and as such has been. Values used for $V_c(0)$ varied geographically based on the sediment structure as shown in Figure 3 and ranged from 1512 to 1750 m/s.

B. SHEAR WAVE EFFECTS

Shear waves are important when considering underwater acoustic propagation because compressional waves can be partially converted to shear waves or Stoneley waves at reflection boundaries. When this occurs, the water borne geoacoustic energy at a receiving hydrophone is rapidly attenuated (Hamilton, 1980). Shear wave effects are generally neglected in many propagation models because it is assumed that the shear wave speed is much less than the speed of sound in water and any effects caused by shear wave propagation can be treated as perturbations (Ellis and Chapman, 1985; Jensen, 1992). Previous experimental results indicated that the excessive low frequency losses observed in some shallow water environments could not be explained via a 'fluid' sediment model. One approach to solve this problem was to include the elasticity of the sedimentary materials and therefore allow for the coupling of acoustic energy into shear waves in the seabed material (Jensen, 1991). Akal and Jensen (1983) earlier pointed out that shear rigidity is a fundamental property of ocean bottom sediments and must be

30

included in a realistic model of the seabed. Neglecting shear effects can only be justified for very "soft" unconsolidated sediments like clayey silt in which the shear speeds are low, less than 200 m/sec (Akal and Jensen, 1983). Kristensen and Hovem (1991) concluded that for a homogeneous bottom the loss due to shear conversion is only important when the shear speed is higher than 400 m/s, a condition normally associated with consolidated sedimentary materials.

Ellis and Chapman (1985) cite an example of underwater acoustic propagation over a chalk bottom where the shear wave speeds were of the order of 1000 m/s. These high shear speeds resulted in acoustic energy being attenuated with range at a rate in excess of that caused by spherical spreading. Although the shear wave speed was less than the sound speed in water, it was large enough that shear wave losses could not be treated as a perturbation. Utilising data from a transmission loss experiment in an area where a chalk/water interface occurred, Ellis and Chapman described a loss regime that displayed very high losses below 200 Hz. By introducing a two-layered model that included the chalk bottom shear effects, the authors where able to reproduce the large losses below 200 Hz using the 'DREA' computer model, PROLOS.

Jensen (1991) lends further support to the importance of shear conversion in his discussion of measured Barents Sea transmission loss data which demonstrated unusually high loss for frequencies below 200 Hz. Jensen tested several geoacoustic models using the SAFARI code in order to simulate the measured data. He found that only an elastic bottom with a high shear speed (700 m/s) at the water/bottom interface achieved the correct result.

If the north/south run data (Figure 7b) is closely inspected, a large amount of loss can be observed between 80 and 250 Hz commencing at approximately 12 km. This effect, although not precisely the same as the Ellis/Chapman and Jensen examples, may represent a similar shear effect. The east/west data display no such effect implying the propagation path was entirely over unconsolidated sedimentary material.

C.   ACOUSTIC MODELING TECHNIQUE

If correct analysis and interpretation of experimental acoustic transmission loss data are to be carried out, then particular attention must be paid to the choice of acoustic prediction model employed. For this shallow water regime a variant of the Parabolic Equation (PE) model was used, i.e., the Range-dependent Acoustic Model (RAM), developed by Collins (1993a,1994).

The PE is a very effective method for solving range dependent ocean acoustic problems. With the introduction of the split-step Padé solution and an improved tridiagonal solver for problems involving variable water depth, the efficiency of finite difference PE solutions can be increased by several orders of magnitude (Collins, 1994). The split-step Padé solution is based on rational approximations of the operator that propagates the solution in range. The solution's efficiency is dependent on the range step size and the number of available processors (Collins, 1994). The split-step Padé solution is valid for problems involving wide propagation angles, large depth variations and elastic ocean bottoms (Collins, 1993a).

The RAM model treats the ocean as a series of range-independent regions. The method propagates the solution between each range independent region and applies an amplitude correction at the regional vertical interfaces (Collins, 1993b). Range

32

dependence is handled by applying an energy-conservation correction as the acoustic parameters vary with range. Tridiagonal systems of equations are repeatedly solved to produce the numerical solution of the parabolic wave equation. The improved split-step Padé solution permits arbitrarily large range steps and dense range sampling and is achieved without loosing accuracy or capability (Collins, 1994). Although the full realisation of the efficiency gain requires the use of multi-processor computers, a significant improvement may be gained with only a single processor computer (Collins, 1993a).

RAM, based on the split-step Padé solution, is a FORTRAN based code and is a variant of the Finite Element Parabolic Equation (FEPE) model. Several variants have been developed and include RAM version 1.2 which is a single processor version, RAM version 1p which is the multiprocessor version and RAMS version 1.2 which is a prototype that treats the ocean bottom as an elastic medium such that shear wave propagation may be accounted for. This study employs the use of RAM 1.2 and RAMS 1.2.

RAM 1.2 provides a fully coherent solution to the acoustic pressure field in an ocean overlying a sediment that supports only propagation of compressional waves (Collins, 1998). RAM requires the following environmental inputs (Fabre, 1997);

    a.   sound speed (m/s) in the water column as a function of depth,

    b.   compressional wave speed (m/s) in the sediment as a function of depth,

    c.   density (g/cm^3) in the sediment as a function of depth, and

    d.   attenuation (dB/λ) in the sediment as a function of depth.

The Appendix details the geoacoustic models used for the east/west and north/south RAM 1.2 runs.

RAMS 1.2 is still under development and as such remains a prototype (Collins, 1999). It treats the bottom as an elastic medium which gives it the capability of modeling shear wave coupling. The model, as it currently exists, can produce unstable results. It is sensitive to the number of Padé approximations selected as well as the range and vertical length steps used (King, 1999). Despite these shortcomings, D. King (NRL Stennis, 1999), has been able to successfully utlise RAMS to match transmission loss curves from various sites around the world where shear wave coupling is known to be a dominant contributor. In addition to the input requirements of RAM, RAMS 1.2 requires the shear speed gradient and shear attenuation gradient.

V. MODEL RESULTS

RAM 1.2 was initially used to model both the east/west and north/south SWISS 1 runs in an attempt to simulate the experimental transmission loss results. Using the limited geoacoustic data provided by DSTO a first guess sediment environment was established. This environment was then intuitively modified using an iterative method, to increase the transmission loss i.e., treating this as an inverse technology problem until a close correlation between the recorded transmission loss data and the model results was achieved. A total of five iterations were needed to achieve a satisfactory simulation for the east/west run. The surface compressional wave speed environment depicted in Figure 3 was used to produce the final geoacoustic model listed in the Appendix. After reviewing the results for the north/south, run it became apparent that RAM 1.2 was not adequate for the north/south run and RAMS 1.2 was used in an attempt to simulate the suspected shear wave losses.

A. EAST/WEST RUN

Comparisons of the predicted RAM 1.2 transmission loss and the measured SWISS 1 east/west run transmission loss data are shown in Figures 11a through 11f. All six figures indicate a close correlation between the predicted RAM transmission loss curves and the measured transmission loss data. The RAM model has closely simulated the apparent duct leakage associated with the 80 Hz signal (Figure 11a) that was apparent in the measured SWISS 1 transmission loss data as well as simulating 200 Hz (Figure 11c) as the optimum frequency.
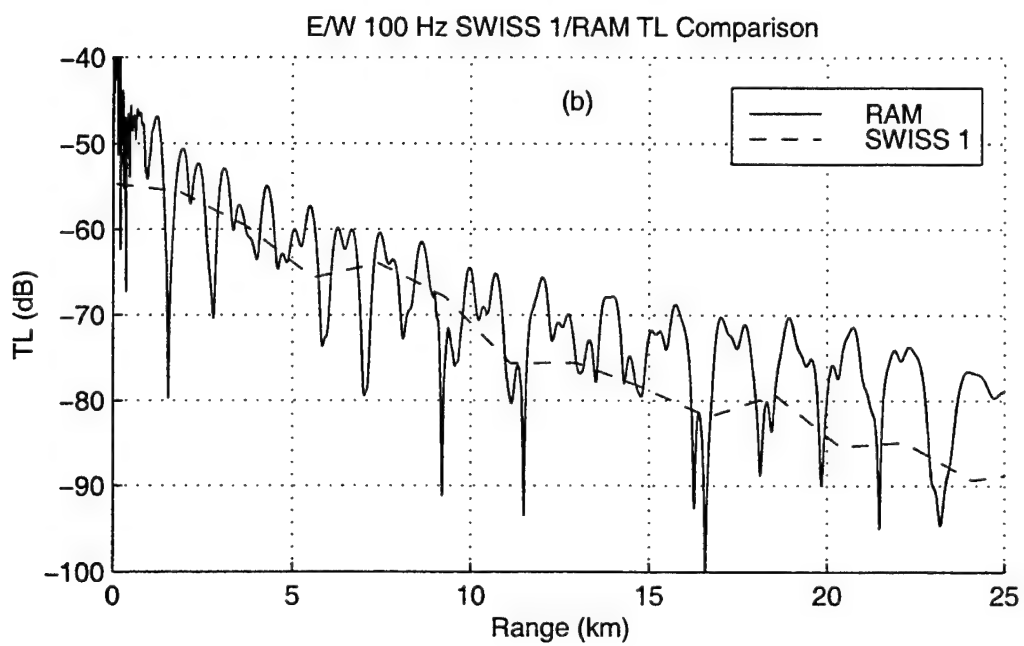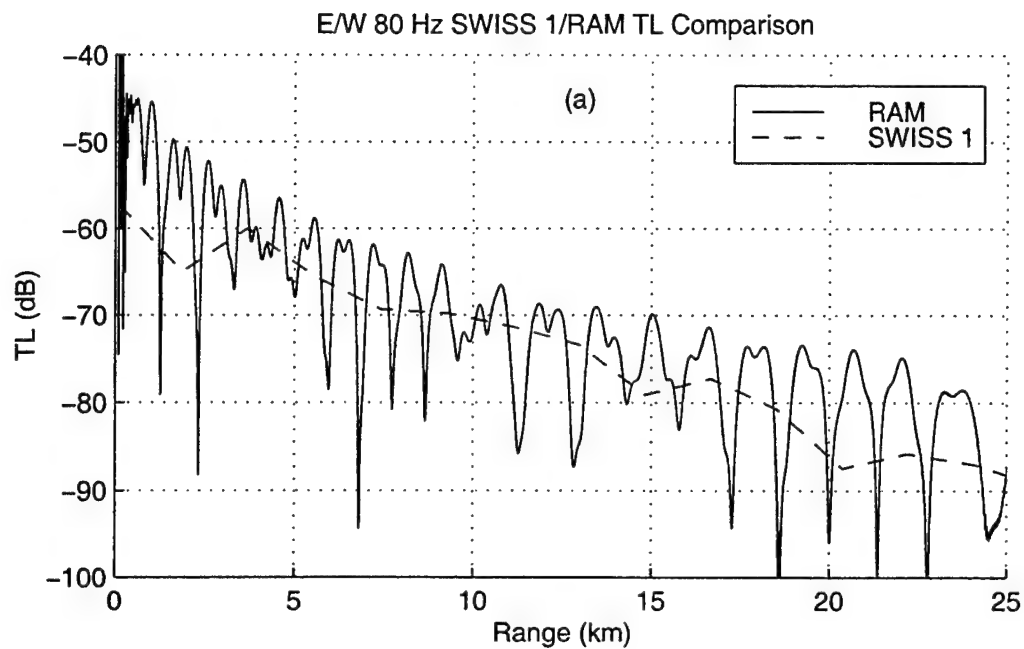
Figures 11a and 11b. A comparison between the RAM 1.2 predicted transmission loss
and east/west SWISS 1 transmission loss data for (a) 80 Hz and (b) 100 Hz.

E/W 200 Hz SWISS 1/RAM TL Comparison

E/W 400 Hz SWISS 1/RAM TL Comparison
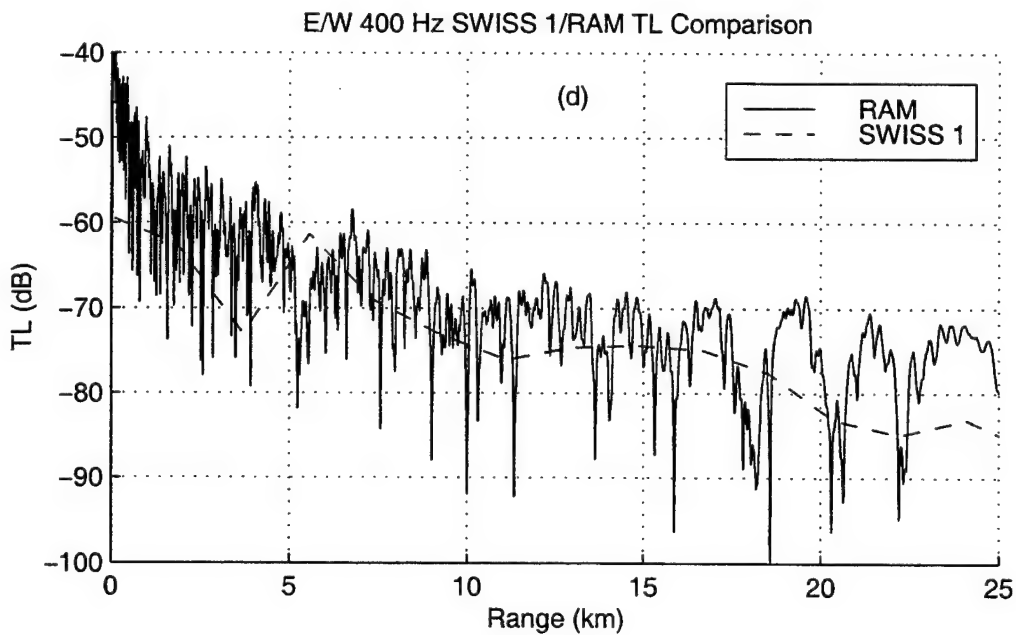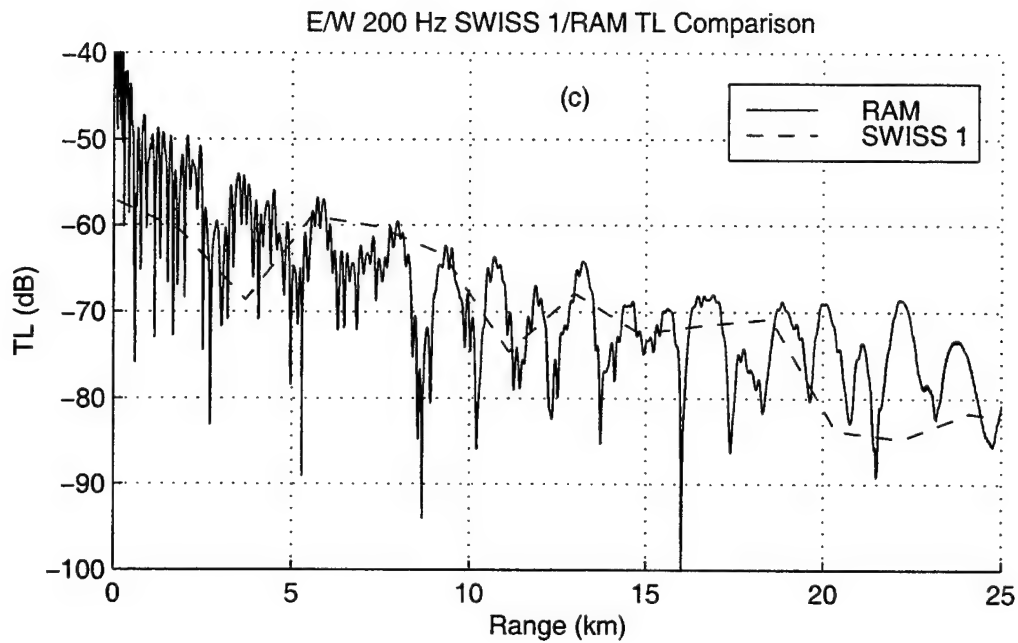
Figures 11c and 11d.   A comparison between the RAM 1.2 predicted transmission loss and east/west SWISS 1 transmission loss data for (c) 200 Hz and (d) 400 Hz.

37

Figures 11e and 11f.   A comparison between the RAM 1.2 predicted transmission loss
and east/west SWISS 1 transmission loss data for (e) 800 Hz and (f) 1250 Hz.

Noting the general lack of geoacoustic data or even site specific data that was available for the SWISS 1 experimental area, coupled with the apparent lack of shear wave effects for the east/west run, RAM 1.2 can be considered to have performed a satisfactory simulation. More exact, range-dependent geoacoustic information would have considerably improved the phase matching of the simulated and measured transmission loss curves.
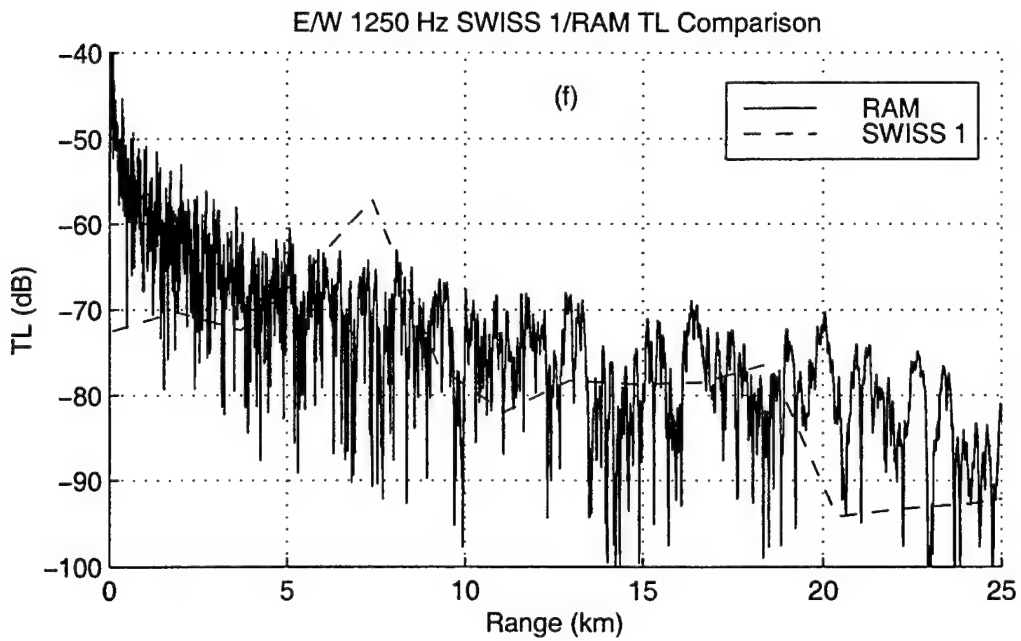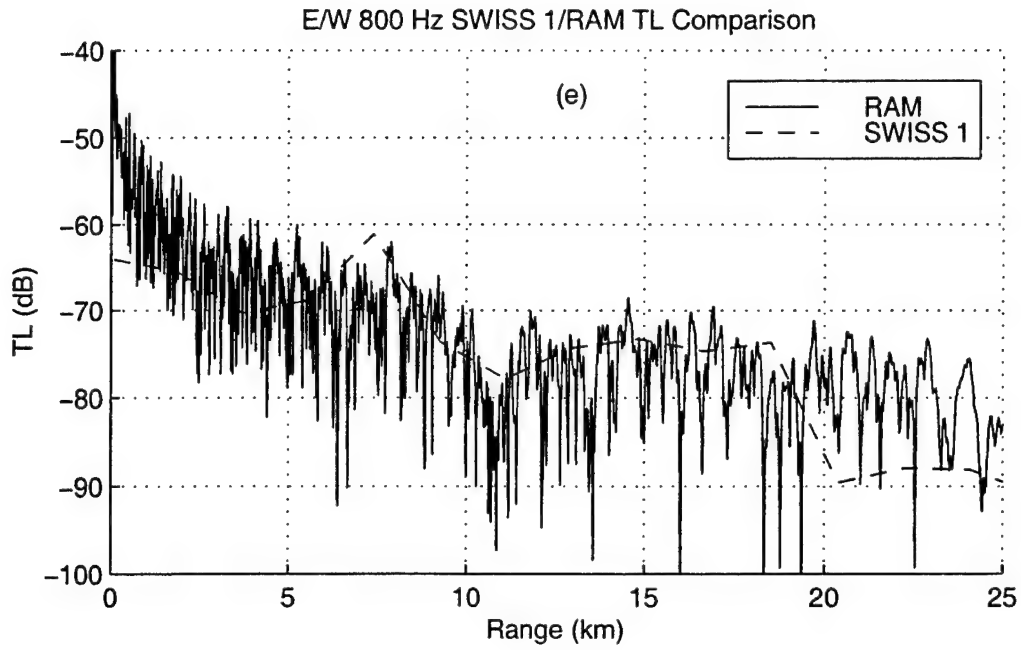
B.   NORTH/SOUTH RUN

Comparisons of the predicted RAM 1.2 transmission loss and the measured SWISS 1 north/south run transmission loss data are shown in Figures 12a through 12f. It is readily apparent that RAM 1.2 considerably underestimated the loss at all frequencies, especially at longer ranges. A close correlation does exist between the RAM data and the measured data for approximately the first 10 kms of each run. After 10 km a marked divergence between the predicted and measured transmission loss data is seen across the frequency spectrum, i.e., the observed data is 20-40 dB lower at 44 km. The start of the divergence coincides with the start of the band pass filtering effect that is observed in Figure 7b. Further iterations were applied to the north/south run sedimentary environment, specifically introducing an extremely high attenuating sediment, in an attempt to reduce the difference between the predicted and measured results. After several iterations the predicted transmission loss was still 15-20 dB less than the measured transmission loss.

Noting the possibility of areas of cemented/consolidated sediments occurring within the experimental area (Strickland, 1999) and the similarities between the case studies detailed by Ellis and Chapman (1985) and Jensen (1991), an investigation into the

39

Figures 12a and 12b.   A comparison between the RAM 1.2 predicted transmission loss and north/south SWISS 1 transmission loss data for (c) 80 Hz and (d) 100 Hz.
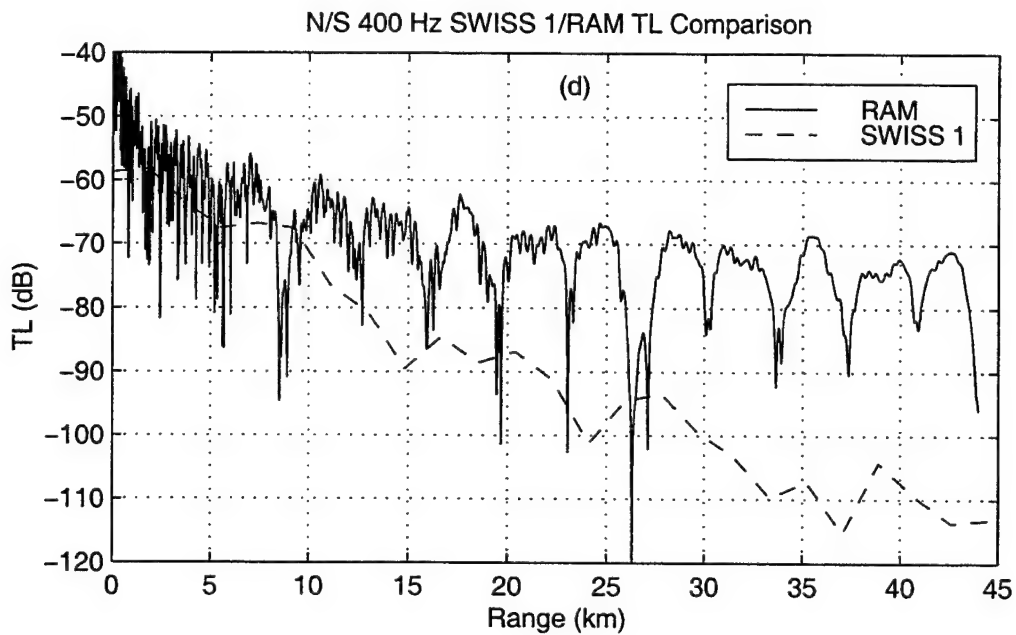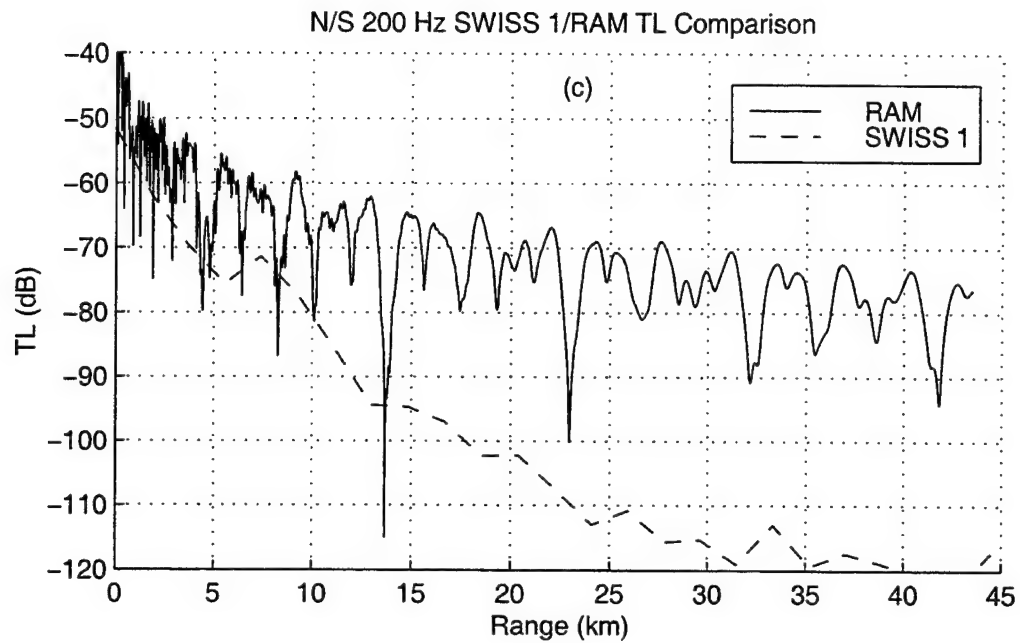
Figures 12c and 12d. A comparison between the RAM 1.2 predicted transmission loss
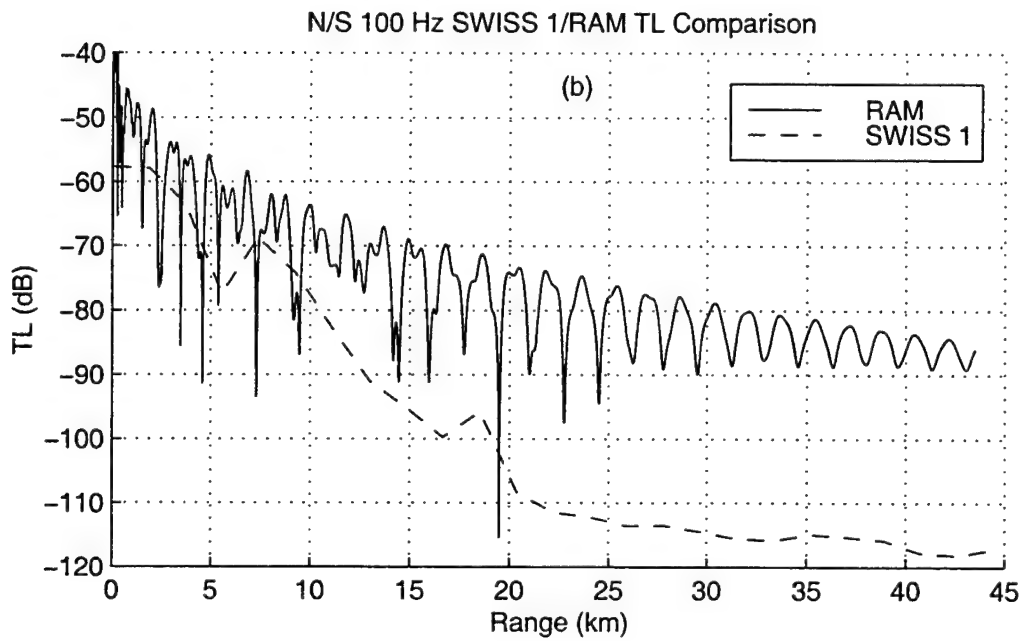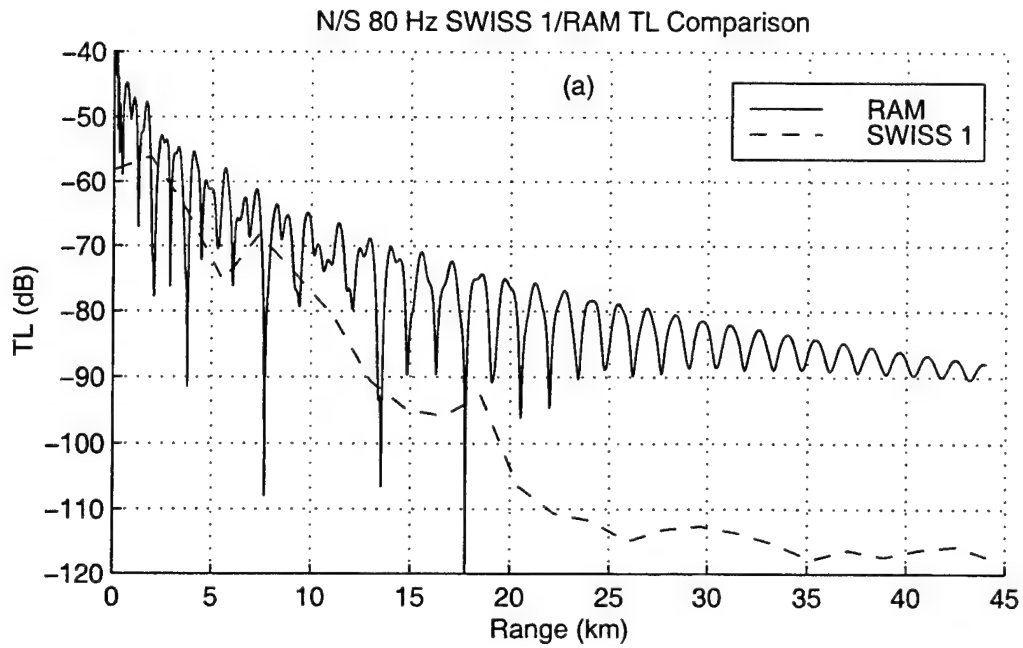and north/south SWISS 1 transmission loss data for (c) 200 Hz and (d) 400 Hz.
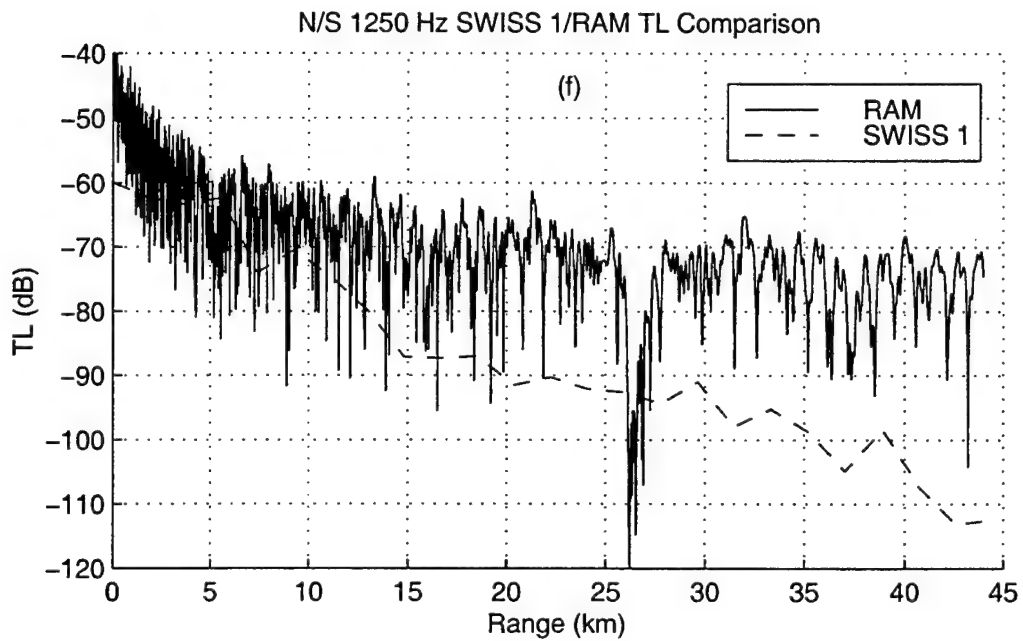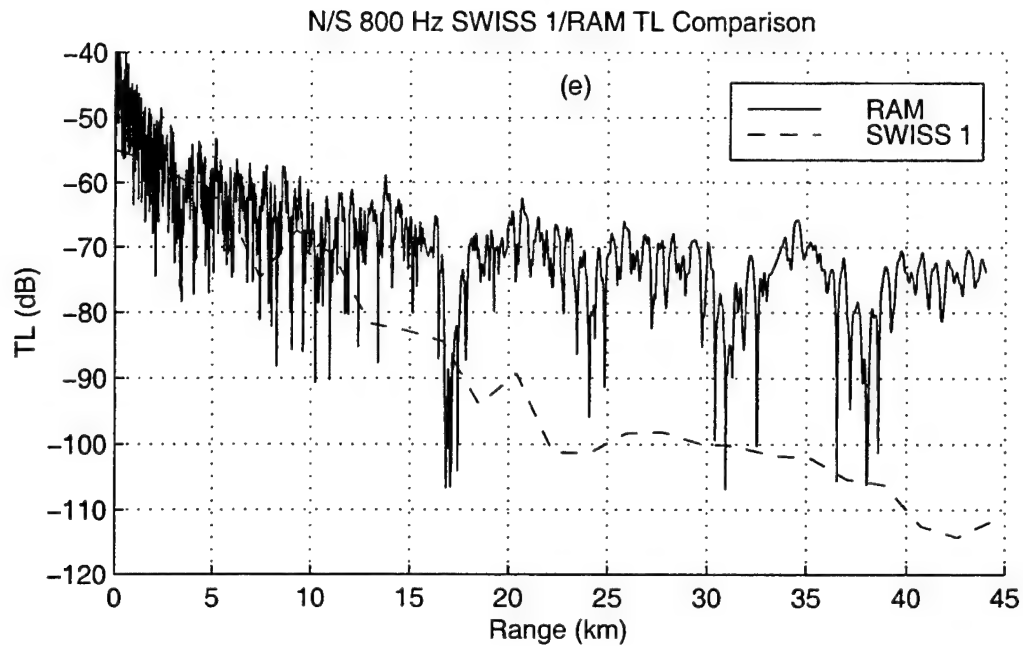
Figures 12e and 12f.   A comparison between the RAM 1.2 predicted transmission loss
and north/south SWISS 1 transmission loss data for (e) 800 Hz and (f) 1250 Hz.

possibility that the large measured transmission losses were a result of shear wave propagation was undertaken. In order to simulate shear wave effects RAMS 1.2 was adopted as the transmission loss model.

King (1999) attempted to incorporate Bishop and O'Brien's (1998) and O'Brien and Wood's (1995) description of the cemented carbonate sediment zones within the Timor Sea into the geoacoustic model detailed in the Appendix in an attempt to derive a representative geoacoustic model for RAMS 1.2. A similar iterative process/inversion technique was used in conjunction with RAMS in an attempt to accurately simulate the measured SWISS 1 transmission loss data. The geoacoustic model that was developed by this iterative process is not unique, rather it is only one of several possible solutions that may work. In fact, the derived geoacoustic model will only produce accurate simulations when used with RAMS (King,1999). After over thirty iterations King was able to produce matches between the model output and the measured data (Figures 13a through 13f). However, he was unable to produce matches for high frequencies, above 500 Hz, and low frequencies, 20 Hz and below (Figure 14). King attributed the limited success of RAMS 1.2 to the following;

a.   the geology within the experimental area is very range dependent, especially in a N/S direction, and

b.   not enough geoacoustic data is available to describe the area adequately.

Although the measured SWISS 1 north/south transmission loss data was not fully simulated, the limited success achieved indicates that shear wave effects do contribute significantly to the large observed transmission losses. Due to the limited geoacoustic database available for the experimental area the only available means to determine a

43

representative geoacoustic model was by iterative processes (King, 1999). This process

is both time consuming and dependent on a foreknowledge of the geological environment

and as such does not lend itself to a rapid resolution of complex geological environments.

In other words, for shallow continental shelf regions which contain outcroppings of

consolidated sedimentary material, a feature that may well be widespread over many

shelf areas, the simple and readily available transmission loss models in use by naval

USW forces are not satisfactory to resolve the transmission loss picture.

Figures 13a and 13b. A comparison between the RAMS 1.2 predicted transmission loss and north/south SWISS 1 transmission loss data for (a) 63 Hz and (b) 100 Hz.
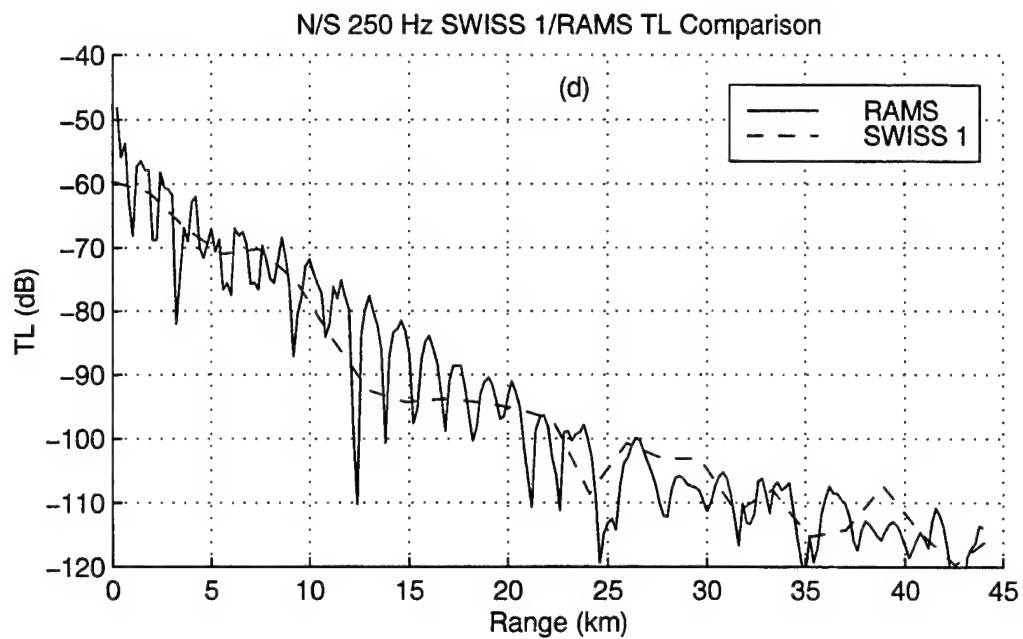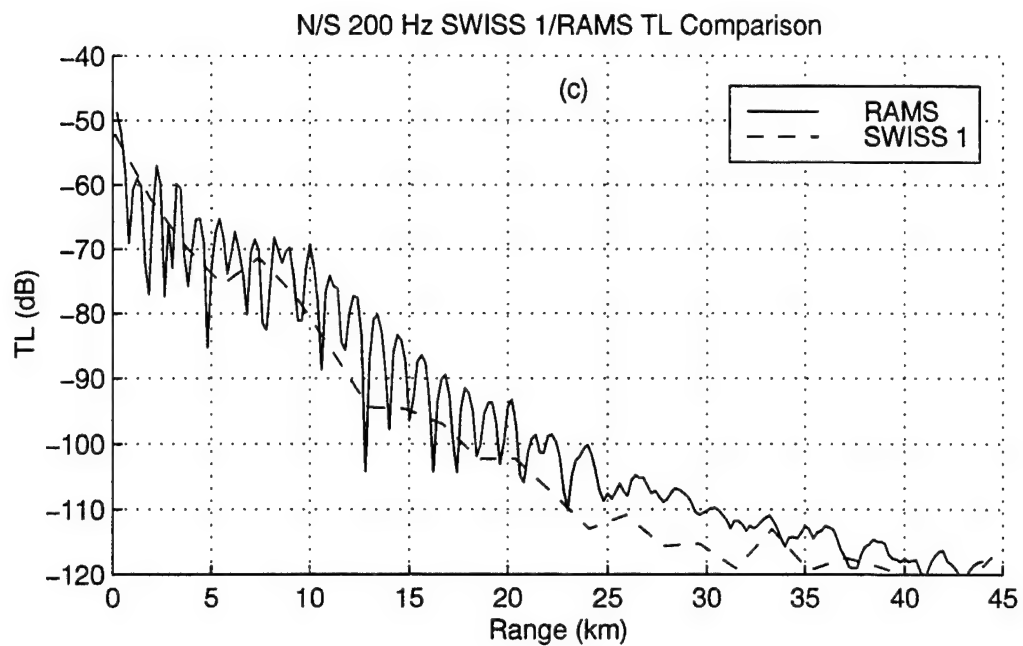
Figures 13c and 13d. A comparison between the RAMS 1.2 predicted transmission loss and north/south SWISS 1 transmission loss data for (c) 200 Hz and (d) 250 Hz.
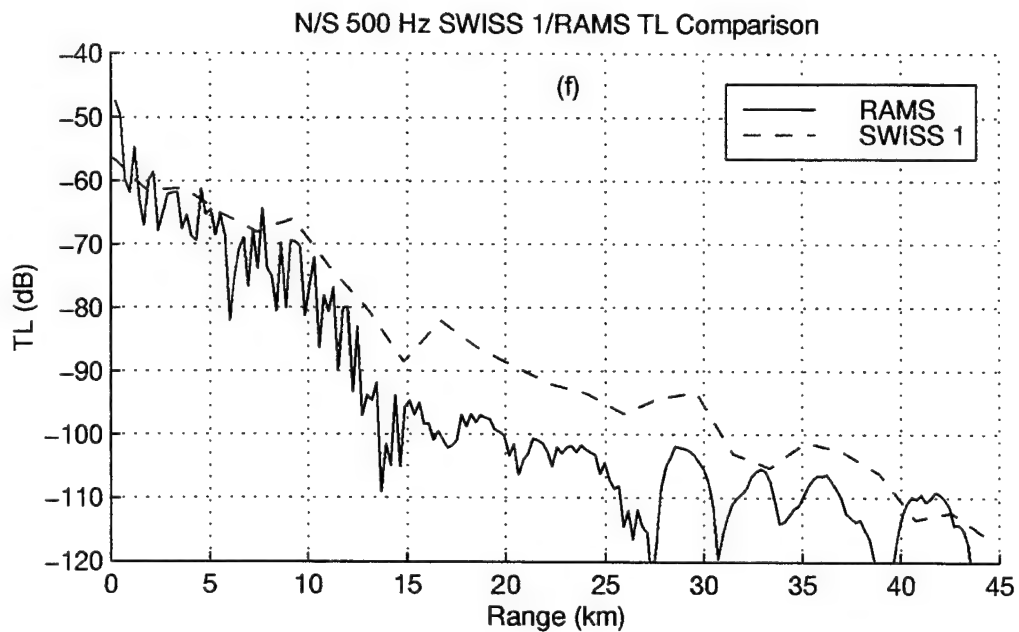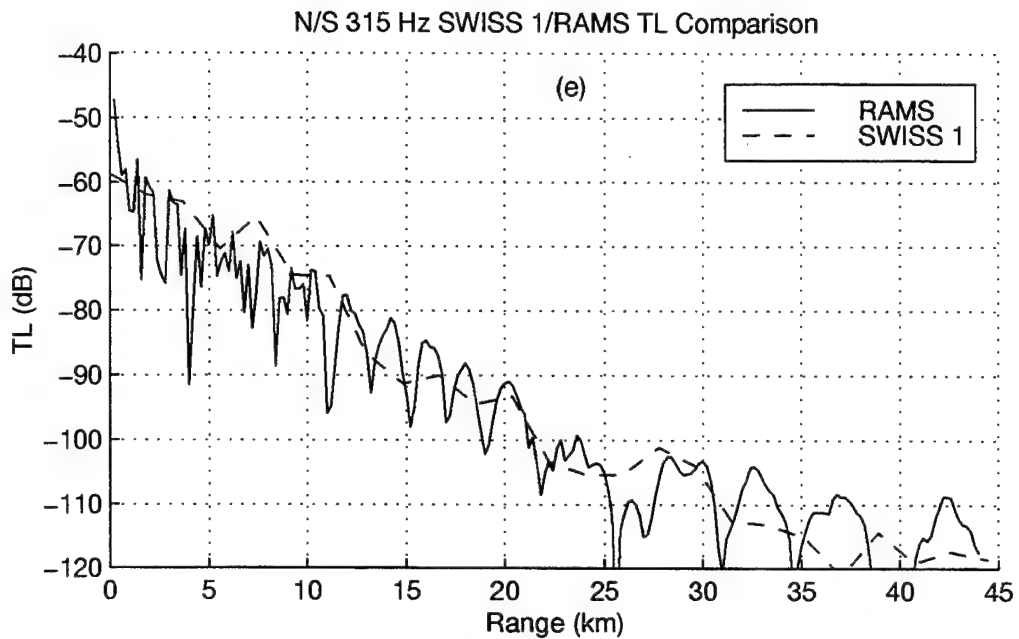
Figures 13e and 13f. A comparison between the RAMS 1.2 predicted transmission loss and north/south SWISS 1 transmission loss data for (e) 315 Hz and (f) 500 Hz.
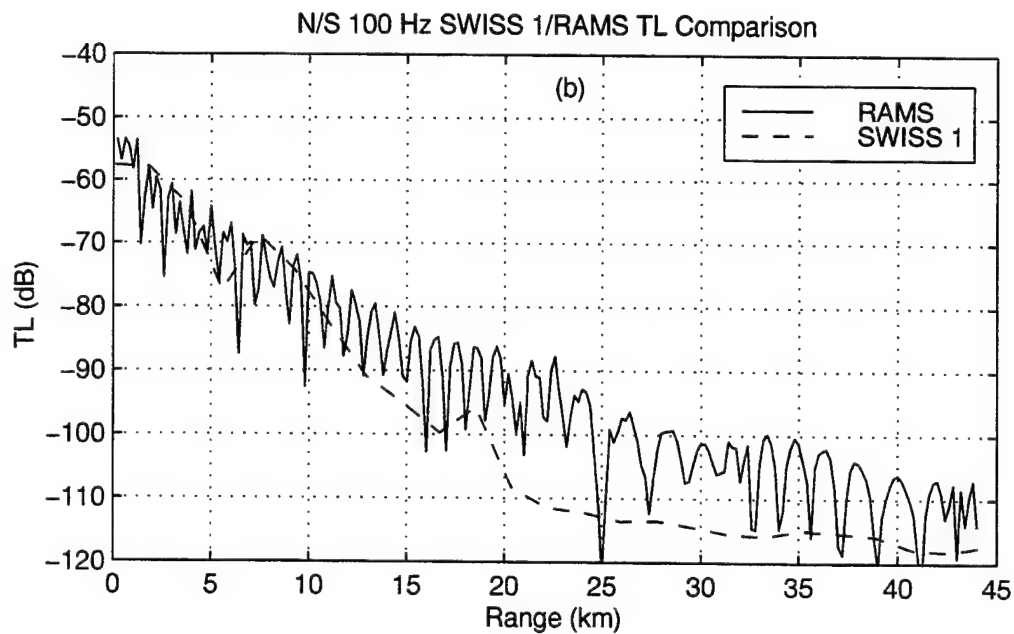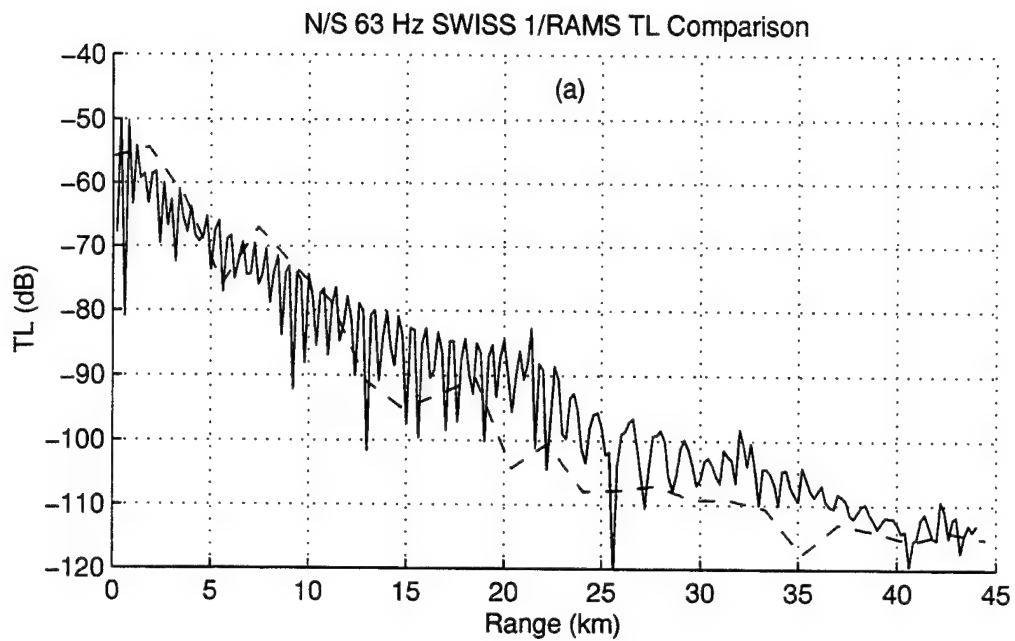
47
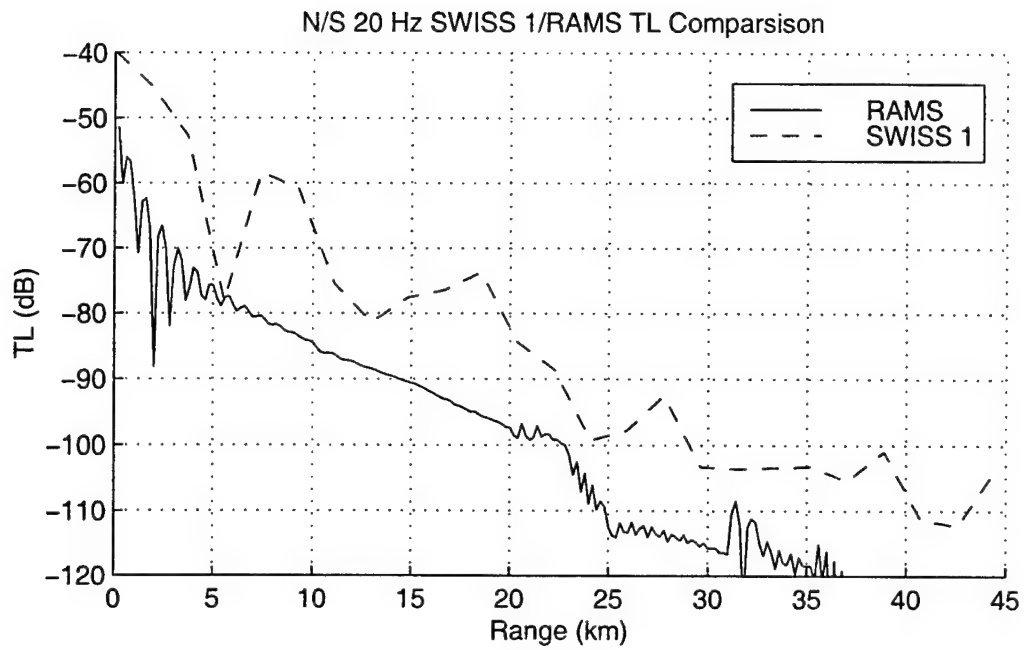
Figure 14.   A comparison between the RAMS 1.2 predicted transmission loss and north/south SWISS 1 transmission loss data for 20 Hz.

VI. DISCUSSION

A comparison of the SWISS 1 north/south and east/west runs and the COOK transmission loss data reveals that the Timor Sea is a highly variable acoustic transmission loss environment. A dramatic indication of the scale of variability was experienced during the SWISS 1 experiment. By simply altering the sound propagation axis by 90^0 a significant difference in the total transmission loss between the two runs was recorded. The east/west track displayed a transmission loss environment that was slightly less than spherical spreading with an optimum frequency approximately centered at 200 Hz. Conversely, the north/south run demonstrated a significantly greater loss environment (approaching 40 log r in some locations) which partial evidence suggests is conducive to coupling of compressive wave energy into shear wave energy. For example, the 200 Hz north/south run displayed a transmission loss 25 dB greater than the east/west run at 20 km.

The COOK data shows a low frequency ($\leq$ 315 Hz) transmission loss dependence similar to the SWISS 1 east/west run but displays a far greater loss at higher frequencies than either SWISS 1 run. The observed variation between the COOK data and the SWISS 1 data may be a result of the different experimental equipment used, i.e., smaller SUS charges and different receivers or may indicate the presence of a third acoustic propagation environment that differs from the two defined by the SWISS 1 experiment.

In spite of the fact that the Timor Sea is an area that has undergone extensive oil and gas exploration, little is documented on the near-surface geological makeup of the Sahul shelf region (Winter, 1998; Strickland, 1999; Jones, 1998; Carter et al., 1992). The lack of detailed specifics concerning the distribution (lateral and vertical),

49

composition and anomalies of the near-surface sediments (upper 100 m) is a critical

shortcoming, especially when considered in conjunction with the demonstrated variability

in acoustic transmission loss along the north/south path. Lack of adequate geoacoustical

data required over thirty iterations of the geoacoustic environment to be implemented in

RAMS 1.2 model runs to achieve any measure of comparability with the observed data.

Even then, satisfactory simulations could only be achieved for frequencies between 20

Hz and 500 Hz.

The influence that shear wave coupling exerts on acoustic transmission within the

Timor Sea is significant. In the tactical environment it creates acoustic 'black holes' for

frequencies below 315 Hz. Knowing the location (size and three-dimensional

orientation) of these 'black holes' would provide an important tactical advantage to any

vessel engaged in maritime surveillance activities and/or USW. One possible cause for

the shear wave coupling is the cementing of the unconsolidated sediment as a result of

hydrocarbon leakage as described in Section 2B, Chapter II. While this explanation

provides one hypothesis for a mechanism leading to the creation of shear wave coupling,

a detailed study needs to be undertaken if the geological makeup is to be accurately

recorded and an accurate geoacoustic model produced. Without an accurate geoacoustic

model meaningful prediction of the acoustic transmission loss and sonar system

performance will not be possible within the Timor Sea. Without the ability to accurately

predict the performance of USW sensors a significant ability to gain a tactical advantage

in USW operations will have been lost.

RAM 1.2 provided a high degree of correlation between the estimated and

measured transmission loss for the east/west SWISS 1 path but failed to replicate the

north/south SWISS 1 transmission loss data as a result of its inability to incorporate shear wave effects. RAMS 1.2, which includes shear wave propagation, was used with limited success to simulate the north/south transmission loss data. The failure of RAMS 1.2 to fully simulate the north/south transmission loss data is attributed to the poor understanding of the Sahul Shelf near-surface geology and geoacoustic parameters (King, 1999). Ellis and Chapman (1985) and Jensen (1991) provide additional evidence for the need to incorporate shear wave propagation in continental shelf areas. Because adequate data were available, they were able to satisfactorily simulate the effects of shear wave coupling using full wave acoustic transmission loss models. If one assumes that shear wave coupling is a widespread phenomenon throughout the world's shallow water zones, then any acoustic propagation model used in these areas should incorporate shear wave effects. Adoption of such models would require a considerable expansion of geoacoustic databases to include shear wave speeds and attenuation.

THIS PAGE INENTIONALLY LEFT BLANK

VII. CONCLUSION

A series of acoustic experiments were conducted by Australian and US researchers off the northwest coast of Australia in the Timor Sea during 1994, termed SWISS 1 and 2, with the purpose of studying in-situ environmental effects on acoustic transmission. The frequency spectrum used in the experiments ranged from 10 to 1600 Hz. This study focused on the two transmission loss runs recorded during the SWISS 1 experiment which was conducted in the Sahul Shelf area in waters ranging from 60 to 120 m in depth. The objectives of the study were to enhance the understanding of the parameters affecting the local transmission loss area and to conduct a performance analysis of the acoustic model RAM. In addition, transmission loss data from an experiment conducted in 1990, using the RAN's former research vessel COOK, was used as a comparison to the SWISS 1 transmission loss data.

The SWISS 1 and COOK transmission loss data revealed a high degree of lateral variability within the Sahul Shelf. Two possibly three distinctive geoacoustic environments were shown to exist and all three displayed transmission loss on the order of or greater than spherical spreading. Of particular interest was the north/south SWISS 1 transmission loss data which displayed characteristics associated with shear wave coupling which was not observed in either the east/west SWISS 1 data or the COOK data.

Reliable geoacoustic data for the SWISS 1 experimental area is sparse making construction of an accurate geoacoustic model difficult. A geoacoustic model was constructed using limited data provided by DSTO and subsequently used in RAM. Previous research (O'Brien and Woods, 1995; Bishop and O'Brien, 1998) conducted in other geographic areas of the Sahul Shelf indicated the existence of localised areas of

cemented sediments created by vertically leaking hydrocarbons. These areas represented regions of high rigidity and their presence could not be discounted within the SWISS 1 experimental area. These high shear wave speed regions provide a mechanism for shear wave coupling within the Sahul Shelf.

RAM was able to accurately simulate the east/west SWISS 1 transmission loss data. However, it failed to simulate the north/south SWISS 1 transmission loss data because it does not incorporate shear wave coupling in its calculations. The observed shear wave coupling in the north/south SWISS 1 transmission loss data was simulated using RAMS, which does incorporate this feature, with limited success. The full frequency spectrum was unable to be simulated as a result of the high range-dependence of the geoacoustic parameters in association with the inadequate geoacoustic data available (King, 1999).

The Sahul Shelf region is a highly variable acoustic environment which can be attributed to the geological diversity of the region. Localised areas exhibit shear wave coupling effects which have a dramatic effect on acoustic transmission below 315 Hz. The area creates a difficult USW environment that poses significant tactical challenges and requires further study if USW sensors and weapons are to be fully utilised within the region.

APPENDIX
RAM 1.2 GEOACOUSTIC MODELS

North/South Run

Range (km)	Depth (m)	Compressional sound speed (m/s)	Density (gm/cm³)	Compressional wave attenuation (k, Hamilton notation, dB/m/kHz)	Compressional attenuation (dB/λ)
0	70	1750	1.94	0.5	0.77
	80	1756	1.95	0.34	0.52
	90	1762	1.96	0.30	0.46
	110	1773	1.99	0.27	0.42
	150	1797	2.03	0.24	0.37
	230	1845	2.12	0.21	0.32
	320	1900	2.23	0.2	0.31
	570	2064	2.51	0.17	0.26
3	60	1700	1.91	0.5	0.77
	70	1705	1.92	0.34	0.52
	80	1711	1.93	0.30	0.46
	100	1723	1.96	0.27	0.42
	140	1745	2.0	0.24	0.37
	220	1792	2.09	0.21	0.32
	310	1846	2.2	0.2	0.31
	560	2005	2.48	0.17	0.26
9	60	1650	1.83	0.75	1.16
	70	1655	1.84	0.51	0.79
	80	1661	1.85	0.46	0.71
	100	1672	1.88	0.40	0.62
	140	1694	1.92	0.36	0.56
	220	1739	2.01	0.32	0.49
	310	1792	2.12	0.29	0.45
	560	1946	2.4	0.27	0.42
12	60	1600	1.74	0.65	1.00
	70	1605	1.75	0.44	0.68
	80	1611	1.76	0.39	0.60
	100	1621	1.79	0.35	0.54
	140	1642	1.83	0.31	0.48
	220	1687	1.92	0.28	0.43
	310	1738	2.03	0.26	0.40
	560	1887	2.31	0.23	0.36
15	60	1550	1.69	0.38	0.59
	70	1555	1.7	0.25	0.39
	80	1560	1.71	0.23	0.36
	100	1571	1.74	0.21	0.32
	140	1591	1.78	0.18	0.78
	220	1634	1.87	0.16	0.25
	310	1683	1.97	0.15	0.23
	560	1828	2.26	0.13	0.20
18	70	1512	1.69	0.38	0.59

	80	1517	1.7	0.25	0.39
	90	1522	1.71	0.23	0.36
	110	1532	1.74	0.21	0.32
	150	1552	1.78	0.18	0.78
	250	1594	1.87	0.16	0.25
	320	1642	1.97	0.15	0.23
	570	1783	2.26	0.13	0.20
22	60	1512	1.69	0.38	0.59
	70	1517	1.7	0.25	0.39
	80	1522	1.71	0.23	0.36
	100	1532	1.74	0.21	0.32
	140	1552	1.78	0.18	0.78
	220	1594	1.87	0.16	0.25
	310	1642	1.97	0.15	0.23
	560	1783	2.26	0.13	0.20
25	110	1512	1.69	0.38	0.59
	120	1517	1.7	0.25	0.39
	130	1522	1.71	0.23	0.36
	150	1532	1.74	0.21	0.32
	190	1552	1.78	0.18	0.78
	270	1594	1.87	0.16	0.25
	360	1642	1.97	0.15	0.23
	610	1783	2.26	0.13	0.20
30	70	1512	1.69	0.38	0.59
	80	1517	1.7	0.25	0.39
	90	1522	1.71	0.23	0.36
	110	1532	1.74	0.21	0.32
	150	1552	1.78	0.18	0.78
	230	1594	1.87	0.16	0.25
	320	1642	1.97	0.15	0.23
	570	1783	2.26	0.13	0.20
36	90	1550	1.69	0.38	0.59
	100	1555	1.7	0.25	0.39
	110	1560	1.71	0.23	0.36
	130	1571	1.74	0.21	0.32
	170	1591	1.78	0.18	0.78
	250	1634	1.87	0.16	0.25
	340	1683	1.97	0.15	0.23
	590	1828	2.26	0.13	0.20
40	110	1600	1.69	0.38	0.59
	120	1605	1.7	0.25	0.39
	130	1611	1.71	0.23	0.36
	150	1621	1.74	0.21	0.32
	190	1642	1.78	0.18	0.78
	270	1687	1.87	0.16	0.25
	360	1738	1.97	0.15	0.23
	610	1887	2.26	0.13	0.20
42	70	1650	1.74	0.68	1.05
	80	1655	1.75	0.46	0.71
	90	1661	1.76	0.41	0.63
	110	1672	1.79	0.36	0.56
	150	1694	1.83	0.32	0.49
	230	1739	1.92	0.29	0.45
	320	1792	2.03	0.27	0.42
	570	1946	2.31	0.24	0.37

44	90	1690	1.74	0.68	1.05
	100	1695	1.75	0.46	0.71
	110	1701	1.76	0.41	0.63
	130	1712	1.79	0.36	0.56
	170	1735	1.83	0.32	0.49
	250	1782	1.92	0.29	0.45
	340	1835	2.03	0.27	0.42
	590	1993	2.31	0.24	0.37

East/West Run

Range (km)	Depth (m)	Compressional sound speed (m/s)	Density (gm/cm³)	Compressional wave attenuation (k, Hamilton notation, dB/m/kHz)	Compressional attenuation (dB/λ)
0	70	1512	1.69	0.38	0.59
	80	1517	1.7	0.25	0.39
	90	1522	1.71	0.23	0.36
	110	1532	1.74	0.21	0.32
	150	1552	1.78	0.18	0.78
	230	1594	1.87	0.16	0.25
	320	1642	1.97	0.15	0.23
	570	1783	2.26	0.13	0.20
3	70	1512	1.69	0.38	0.59
	80	1517	1.7	0.25	0.39
	90	1522	1.71	0.23	0.36
	110	1532	1.74	0.21	0.32
	150	1552	1.78	0.18	0.78
	230	1594	1.87	0.16	0.25
	320	1642	1.97	0.15	0.23
	570	1783	2.26	0.13	0.20
9	70	1550	1.77	0.68	1.05
	80	1555	1.78	0.25	0.71
	90	1560	1.79	0.23	0.63
	110	1571	1.82	0.21	0.56
	150	1591	1.86	0.18	0.49
	230	1634	1.95	0.16	0.45
	320	1683	2.06	0.15	0.42
	570	1828	2.34	0.13	0.37
15	95	1600	1.86	0.68	1.05
	105	1605	1.87	0.25	0.71
	115	1611	1.88	0.23	0.63
	135	1621	1.9	0.21	0.56
	175	1642	1.95	0.18	0.49
	255	1687	2.04	0.16	0.45
	345	1738	2.15	0.15	0.42
	595	1887	2.43	0.13	0.37
18	90	1650	1.89	0.55	0.85
	100	1655	1.90	0.37	0.57
	110	1661	1.91	0.33	0.51
	130	1672	1.94	0.30	0.46
	170	1694	1.98	0.26	0.40
	250	1739	2.07	0.24	0.37
	340	1792	2.18	0.22	0.34
	590	1946	2.46	0.19	0.29
22	85	1700	1.94	0.5	0.77
	95	1705	1.95	0.34	0.52
	105	1711	1.96	0.3	0.46
	125	1723	1.99	0.27	0.42
	165	1745	2.03	0.24	0.37
	245	1792	2.12	0.21	0.32
	335	1846	2.23	0.20	0.31

	585	2005	2.51	0.18	0.28
25	120	1700	2.03	0.48	0.74
	130	1705	2.04	0.33	0.51
	140	1711	2.05	0.29	0.45
	160	1723	2.08	0.26	0.40
	200	1745	2.12	0.23	0.36
	280	1792	2.21	0.21	0.32
	370	1846	2.32	0.19	0.29
	620	2005	2.6	0.17	0.26

THIS PAGE INTENTIONALLY LEFT BLANK

LIST OF REFERENCES

T. Akal and F.B. Jensen, "Effects of Sea-Bed on Acoustic Propagation," in Acoustics and the Seabed: Conference Proceedings, edited by N.G Pace, Bath University, Bath, 225-232, 1983.

D.J. Bishop and G.W. O'Brien, "A Multi-Disciplinary Approach to Definition and Characterisation of Carbonate Shoals, Shallow Gas Accumulations and Related Complex Near-Surface Sedimentary Structures in the Timor Sea," Australian Petroleum Production and Exploration Association Journal, 93-113, 1998.

Bureau of Meteorology (BOM), "Monthly Weather Review, Northern Territory, March 1994," Australia, 1994.

R.L. Carlson, A.F. Gangi and K.R. Snow, " Empirical Reflection Travel Time Versus Depth and Velocity Versus Depth Functions For the Deep-Sea Sediment Column," J. Geophys. Res., 91, 8249-8266, 1986.

J. Carter, M.V. Hall and S. Prenc, "Shallow Water Transmission Experiments in the Timor and Arafura Seas," Technical Report MRL-TR-x/92 (draft), Defence Science and Technology Organisation, Australia, March, 1992.

M.D. Collins, "A Split-Step Pade Solution for the Parabolic Equation Method," J. Acoust Soc. Am, 93(4), Pt 1, 1993a.

M.D. Collins, "An Energy-Conserving Parabolic Equation for Elastic Media," J. Acoust Soc. Am, 94(2), Pt. 1, 1993b.

M.D. Collins, "Generalization of the Split-Step Pade Solution," J. Acoust Soc. Am, 96(1), 1994.

M.D. Collins, "User's Guide for RAM Versions 1.0 and 1.0p," Naval Research Laboratory, Washington, DC., 1998.

M.D. Collins, Personal communications, NRL-Stennis, 1999

G. Creswell, A. Frische, J. Peterson and D. Quadfasel, "Circulation in the Timor Sea," J. Geophys. Res., 98(C8), 14379-14389, 1993.

J. Dunlop, "Acoustic Properties of Marine Sediments," J. Acoustics Australia, 20(3), 81-85, 1992.

D.D. Ellis and D.M.F. Chapman, "A Simple Shallow Water Propagation Model Including Shear Wave Effects," J. Acoust. Soc. Am., 78(6), 2087-2095, 1985

J.P. Fabre, "RAM User's Guide," Neptune Sciences, Inc, Slidel, MS,1997.

E.A. Hamilton, " Geoacoustic Modeling of the Sea Floor," J. Acoust. Soc. Am., 68(5), 1313-1340, 1980.

E.A. Hamilton, "Sound Velocity as a Function of Depth in Marine Sediments," J. Acoust. Soc. Am., 78(4), 1348-1355, 1985.

E.A. Hamilton and R. T. Bachman, " Sound Velocity and Related Properties of Marine Sediments," J. Acoust. Soc. Am., 72(6), 1891-1904, 1982.

C.J. Jenkins, "Geological and Geophysical Studies in Support of Acoustic Experiments in the Northeastern Indian Ocean," Ocean Sciences Institute Report No. 42, University of Sydney, Sydney, March 1991.

F.B. Jensen, "Excess Attenuation in Low-Frequency Shallow-Water Acoustic: A Shear Wave Effect?," in Shear Waves in Marine Sediments, edited by J. M. Hovem, M.D. Richardson and R. D. Stoll, Kluwer Academic Publishers, Boston, 421-430, 1991.

A.D. Jones, Personal communication, DSTO, 1998

D. King, Personal communication, NRL-Stennis, 1999.

A. Kristensen and J.M. Hovem, "Sensitivity of Bottom Loss to Attenuation and Shear Conversion," in Shear Waves in Marine Sediments, edited by J. M. Hovem, M.D. Richardson and R. D. Stoll, Kluwer Academic Publishers, Boston, 431-438, 1991.

A. Larsson, "Dividing Australian Shallow Waters into Acoustic Propagation Loss Zones," in International Conference on Underwater Acoustics 5-7 December 1994 held at University of New South Wales, Sydney, 94-96, 1994.

A. Larsson, A. Jones and J. Savage, "SWISS Trial: Results and Interpretation," DSTO Document TTCP GTP-10 (Restricted), (only unclassified data used), 1994.

J.M. Null, R.H. Bourke and J.H. Wilson, "Perturbative Inversion of Geoacoustic Parameters in Shallow Water Environment," IEEE Oceanic Engineering, 21(4), 468-504, 1996.

G.W. O'Brien and E.P. Woods, "Hydrocarbon-related Diagentic Zones (HRDZs) in the Vulcan Sub-basin, Timor Sea: Recognition and Exploration Implication," Australian Petroleum Exploration Association Journal, 220-252, 1995.

G.A. Scanlon, "Estimation of Bottom Scattering Strength from Measured and Modeled AN/SQS-53C Reverberation Levels," ," IEEE Oceanic Engineering, 21(4), 440-451, 1996.

J. Sendt, Personal communications, Thomson Marconi Sonar PTY Limited, Australia, 1999.

R.D. Stoll, "Theoretical Aspects of Sound Transmission in Sediments," J. Acoust Soc Am., 68(5), 1341-1349, 1980.

P. Stickland, Personal communication, Senior Geophysicist, Geophysical Technology Group BHP Petroleum, 1999.

J.M. Thorleifson and P.D. Boyle, "Source Level Measurements of 1.8 lb and 1.1 oz Underwater Sound Signals," Unpublished Report, Defence Research Establishment Pacific, B.C., Canada, 1976.

J. Urick, "Principles of Underwater Sound," 3rd ed., McGraw Hill Inc., New York, NY, 1983.

D.E. Weston, "Underwater Explosions as Acoustic Sources" Proc. Phys, Soc., LXXVI, 233-249, 1960.

W. Winter, Personal communications, Santos PTY Limited, Australia, 1998.

THIS PAGE INTENTIONALLY LEFT BLANK

INITIAL DISTRIBUTION LIST

1. Defense Technical Information Center 2
    8725 John J. Kingman Rd., STE 0944
    Ft. Belvoir, Virginia 22060-6218

2. Dudley Knox Library 2
    Naval Postgraduate School
    411, Dyer Rd.
    Monterey, California 93943-5101

3. Maritime Commander Australia 1
    Maritime Headquarters
    1 Wylde St.
    Potts Point, NSW 2011
    Australia

4. Chairman (Code OC/BF) 1
    Department of Oceanography
    Naval Postgraduate School
    Monterey, California 93943-5100

5. Prof. R.H. Bourke (Code OC/BF) 1
    Department of Oceanography
    Naval Postgraduate School
    Monterey, California 93943-5000

6. Dr. J.H. Wilson 1
    Neptune Sciences, Inc.
    3834 Vista Azul
    San Clemente, CA 92674

7. Chief of Staff - Naval Training Command 1
    Naval Training Command Headquarters
    HMAS CERBERUS
    Westernport, VIC 3920
    Australia

8. Dr. A.D. Jones 1
    Aeronautical and Maritime Research Laboratory
    P.O. Box 1500
    Salisbury, SA 5108
    Australia

9. Dr. J. Sendt 1
    Thomson Marconi Sonar
    274 Victoria Rd.
    Rydalmere, NSW 2125
    Australia

10. Director of Oceanography and Meteorology 1
    Maritime Headquarters
    1 Wylde St.
    Potts Point, NSW 2011
    Australia

11. Officer in Charge of the Applied Meteorology and Oceanography Center 1
    Maritime Headquarters
    1 Wylde St.
    Potts Point, NSW 2011
    Australia

12. Naval Space and Warfare Command 1
    PD18
    153560 Hull St.
    San Diego, CA 92152-5002

13. Dr. D. King 1
    Code 7181
    Naval Research Laboratory
    Stennis Space Center,
    MS 39529

14. LCDR S.M. Taylor 1
    Maritime Headquarters
    1 Wylde St.
    Potts Point, NSW 2011
    Australia